

P. Bernardini - Università and INFN, Lecce (Italy)
On behalf of the ARGO-YBJ Collaboration

Les Rencontres de Physique de la Vallée d'Aoste
La Thuile - February 28, 2011



Cosmic Rays in the TeV region with the ARGO-YBJ detector



Outline

✓ Detector features and performance

✓ ~~Gamma Astronomy~~

✓ Cosmic Rays (CR)

Moon shadow & antiproton flux
Anisotropies
Light component spectrum
Proton cross-section
Shower structure

羊八井宇宙线观测站 ARGO

ARGO LABORATORY OF YBJ COSMIC RAY OI

The YangBaJing Cosmic Ray Observatory (Tibet, China)

Altitude 4300 m a.s.l.

Longitude $90^{\circ} 31' 50''$ East

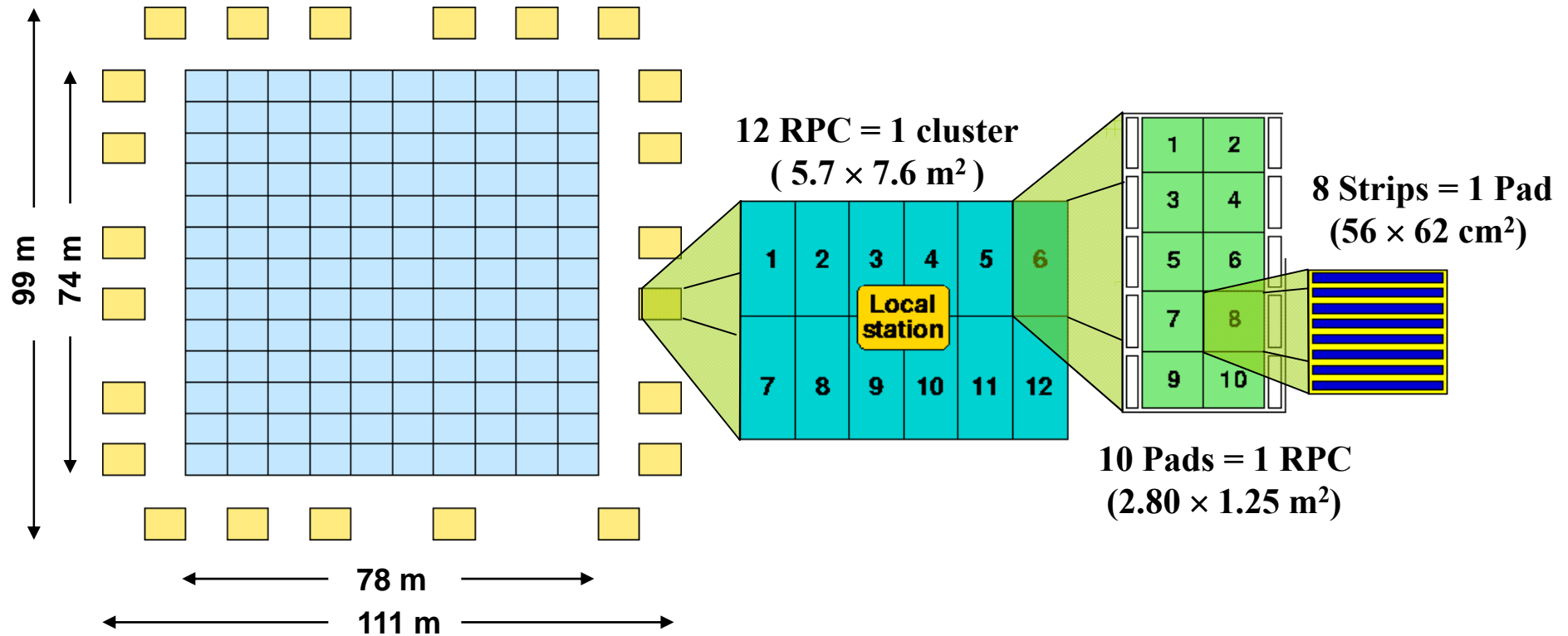
Latitude $30^{\circ} 06' 38''$ North



Astrophysical Radiation
with Ground-based
Observatory at YangBaJing

Tibet AS- γ





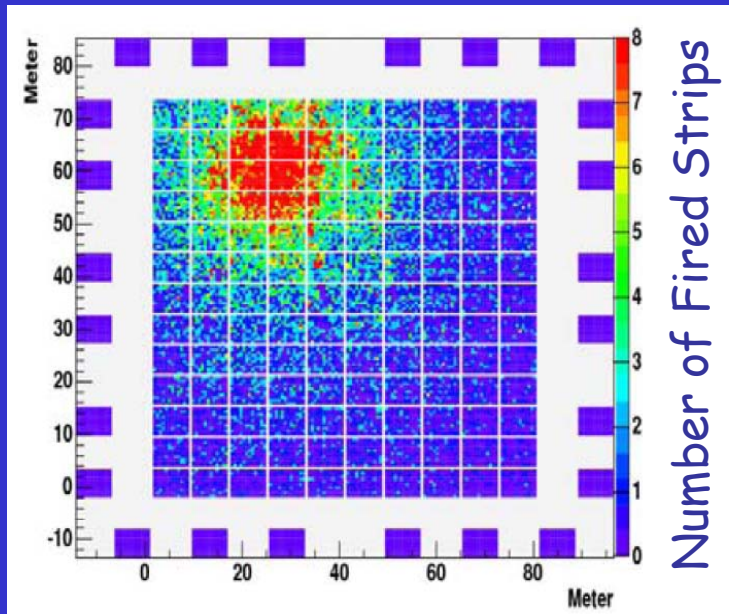
✓ Layer of Resistive Plate Chambers (RPC)

✓ Active area : central carpet ~ 5600 m²
 sampling guard-ring ~ 1000 m²

✓ Data taking : since July 2006 with the central carpet
 since November 2007 with the guard-ring

Analog charge read-out (big-pads) is working





Duty cycle > 85%
Field of View ~ 2 sr

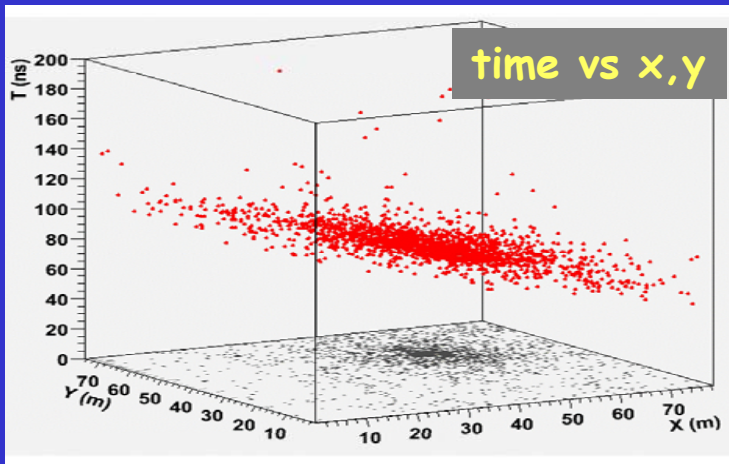
Shower mode

Space pixel: single strip ($7 \times 62 \text{ cm}^2$)

Time pixel: pad ($56 \times 62 \text{ cm}^2$) is the OR of 8 strips, with a resolution of ~1.8 ns

Dynamical range for protons by means of pads, strips and big-pads :

~ 1 - 10^4 TeV



Detection of Extensive Air Showers (direction, size, core ...)

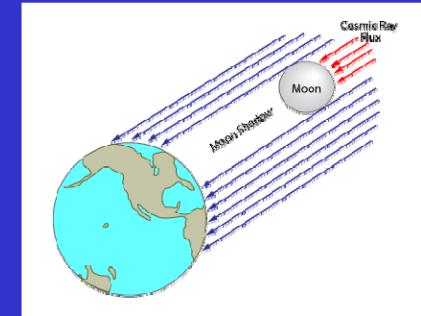
Aims : cosmic-ray physics (threshold ~ 1 TeV)

VHE γ -astronomy (threshold ~ 300 GeV)

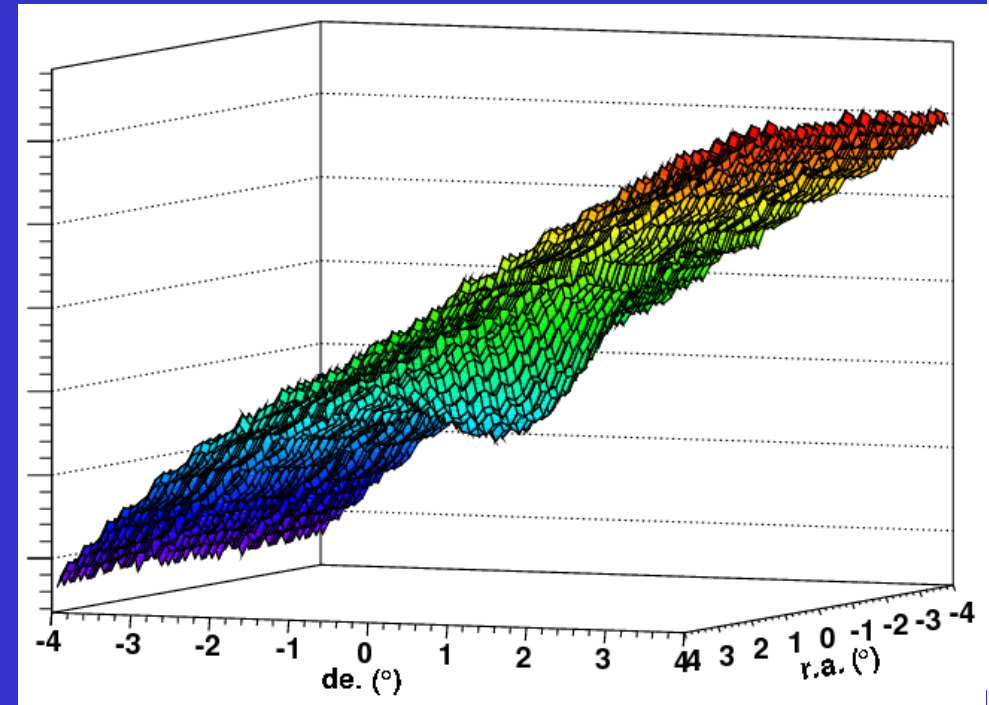
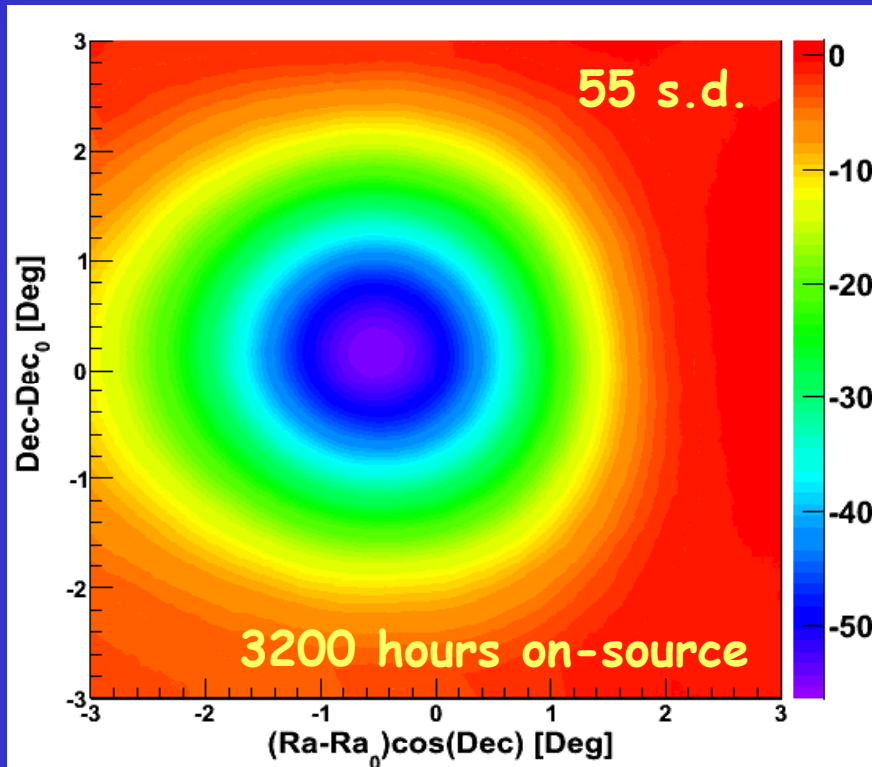


Moon shadow

Moon shadow



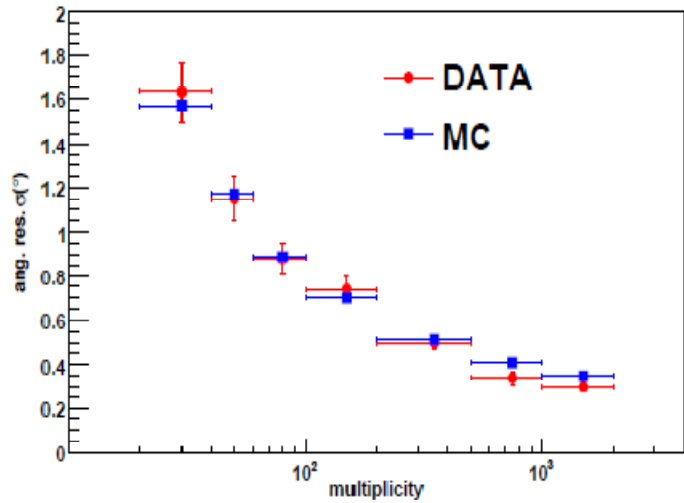
Analysis cuts: $N_{\text{HIT}} > 100$ and $\theta < 50^\circ$



≈ 9 standard deviations / month

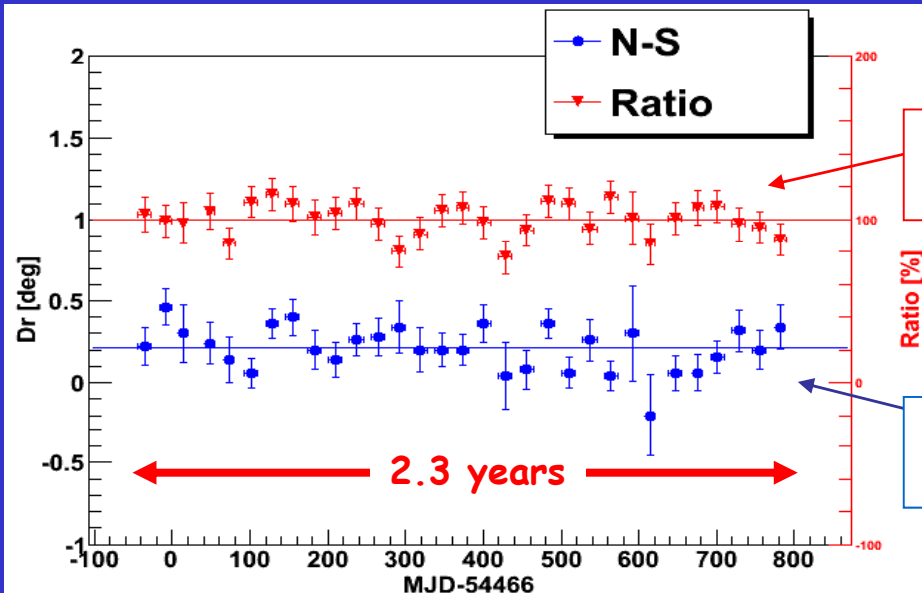
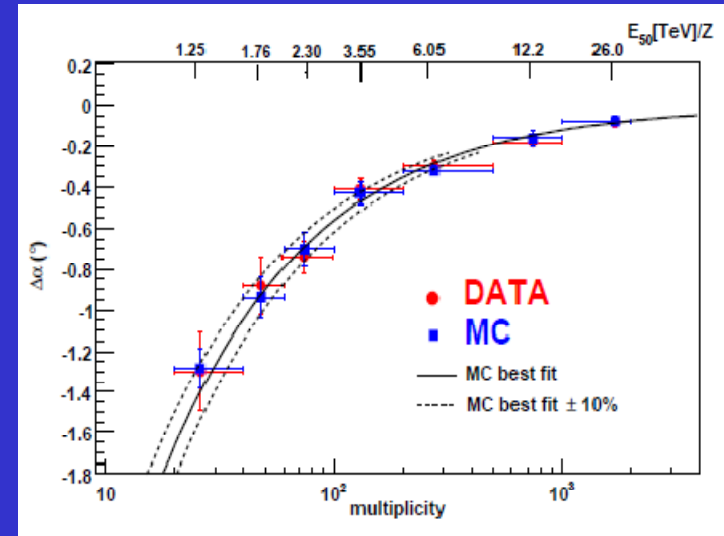
The deficit surface is the convolution of the Point Spread Function of the detector and the widespread Moon disc

$$RMS \simeq \sigma \sqrt{1 + \left(\frac{R}{2\sigma}\right)^2}$$



Angular resolution vs hit multiplicity
(angular resolution \propto deficit depth)

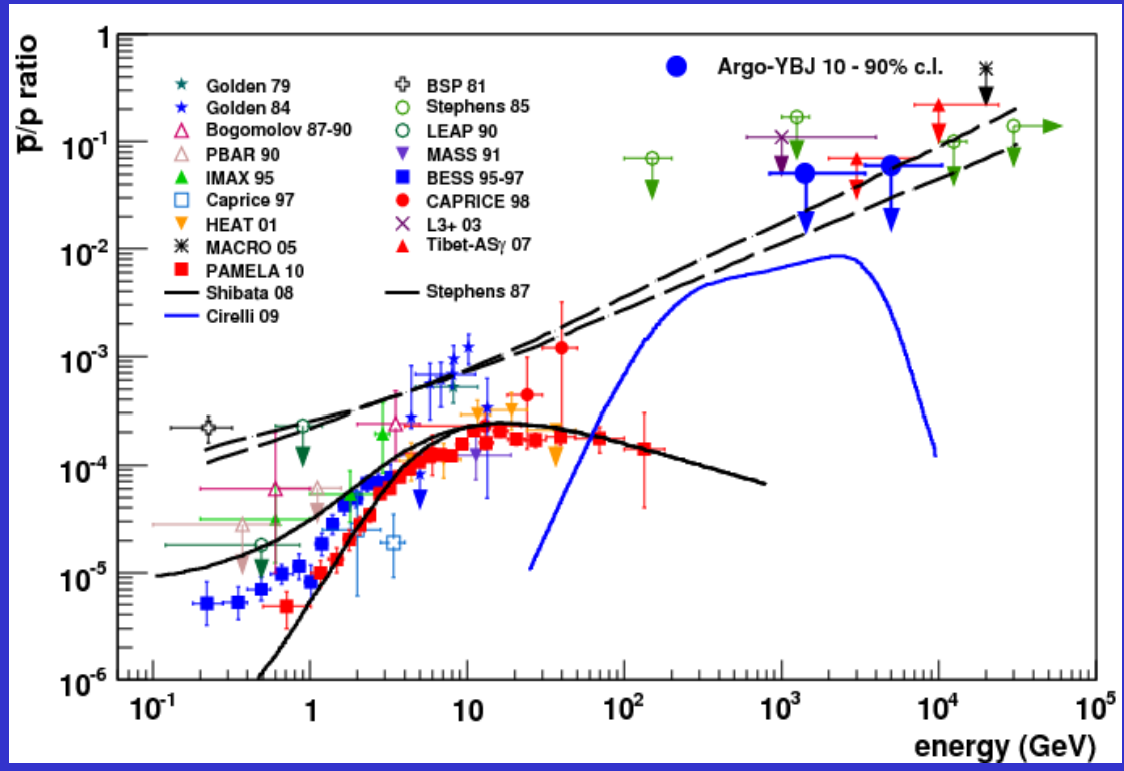
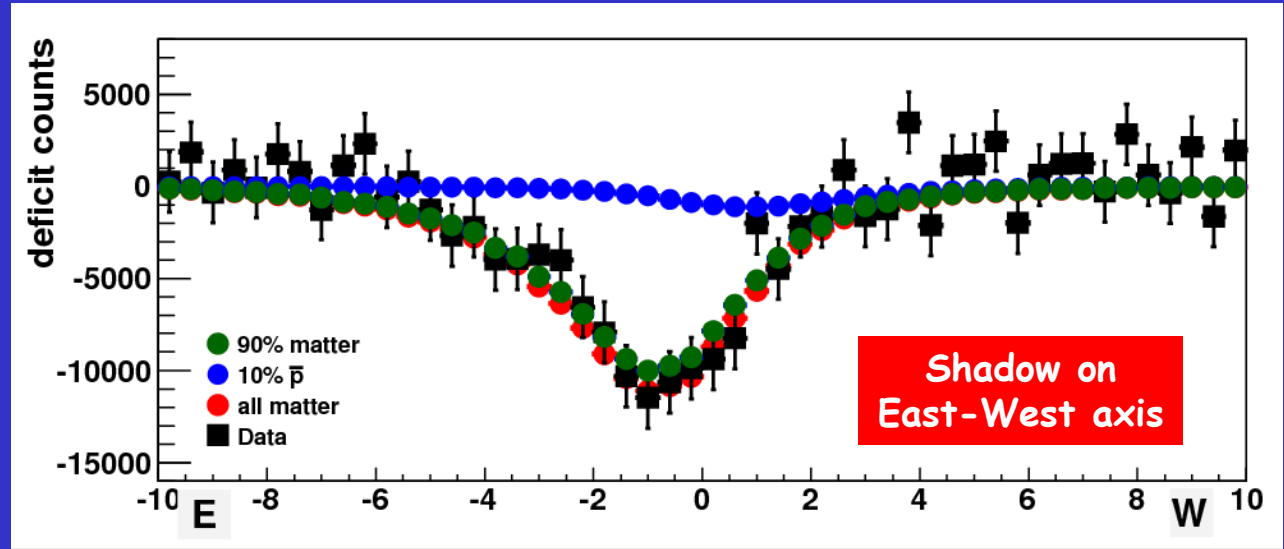
Westward shadow shift
 $\Delta\alpha \approx 1.57^\circ Z / E \text{ (TeV)}$



Ratio of the measured deficit to the expected one

Shift on North-South axis (pointing stability)

Looking for an East deficit as antiproton signal



Maximum Likelihood
+ Feldman & Cousins

Upper limit on
the antiproton flux

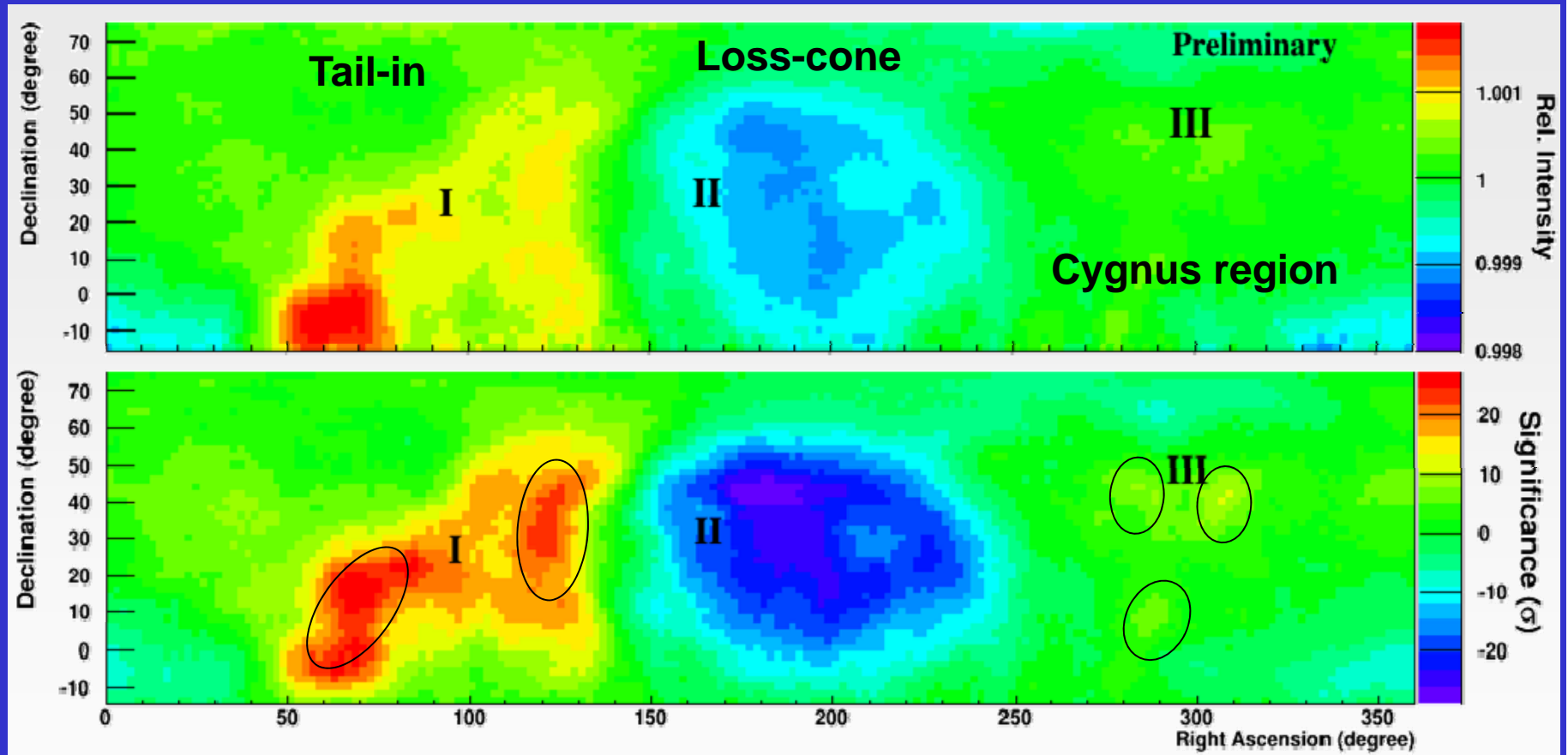


Anisotropies

Large scale CR anisotropy

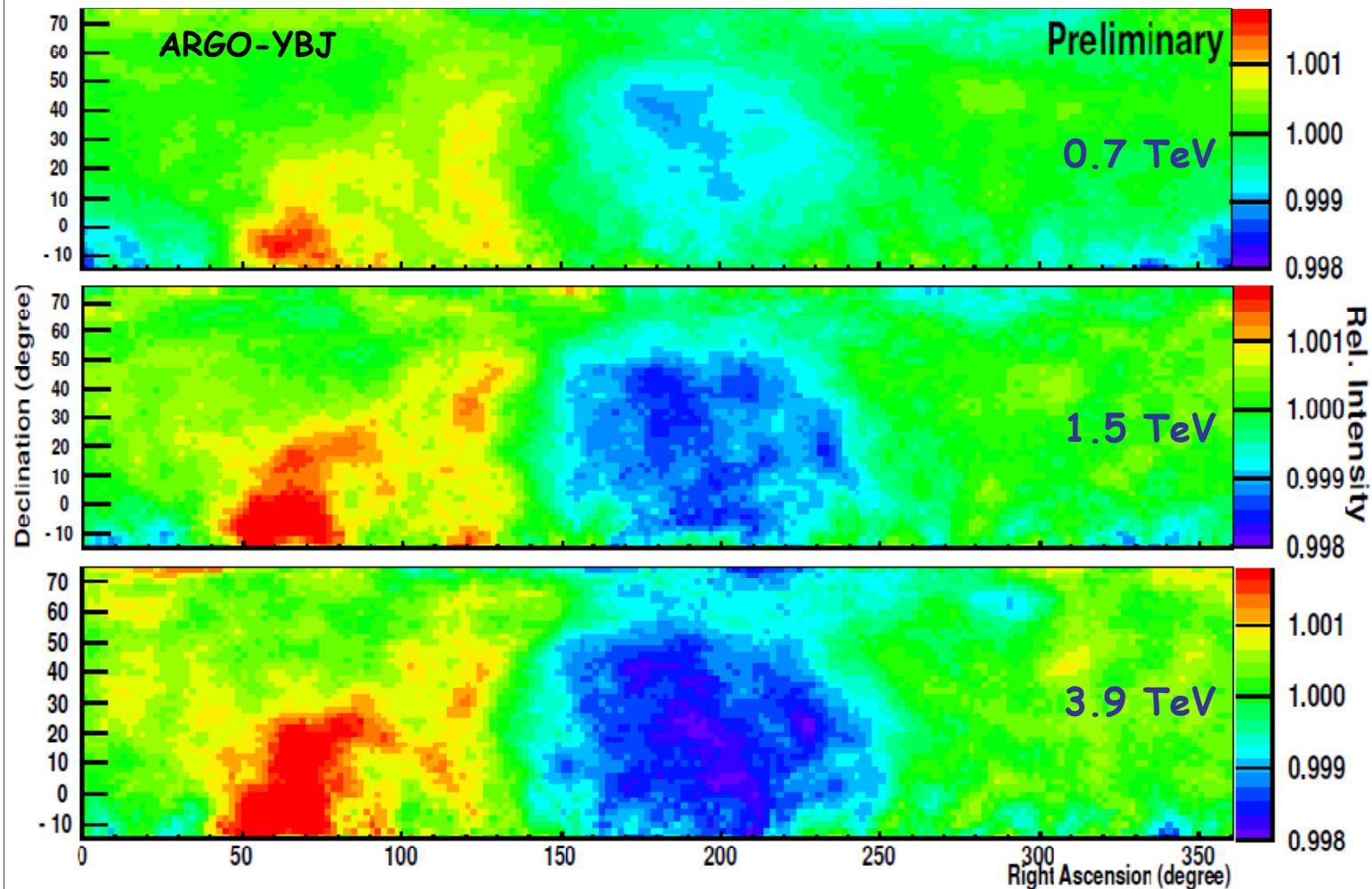
Large statistics and wide Field of View (> 2 sr)
allow the 2-D measurement of the anisotropy

ARGO-YBJ DATA (2008 and 2009) : 130×10^9 events ($E_{50} = 1.1$ TeV)



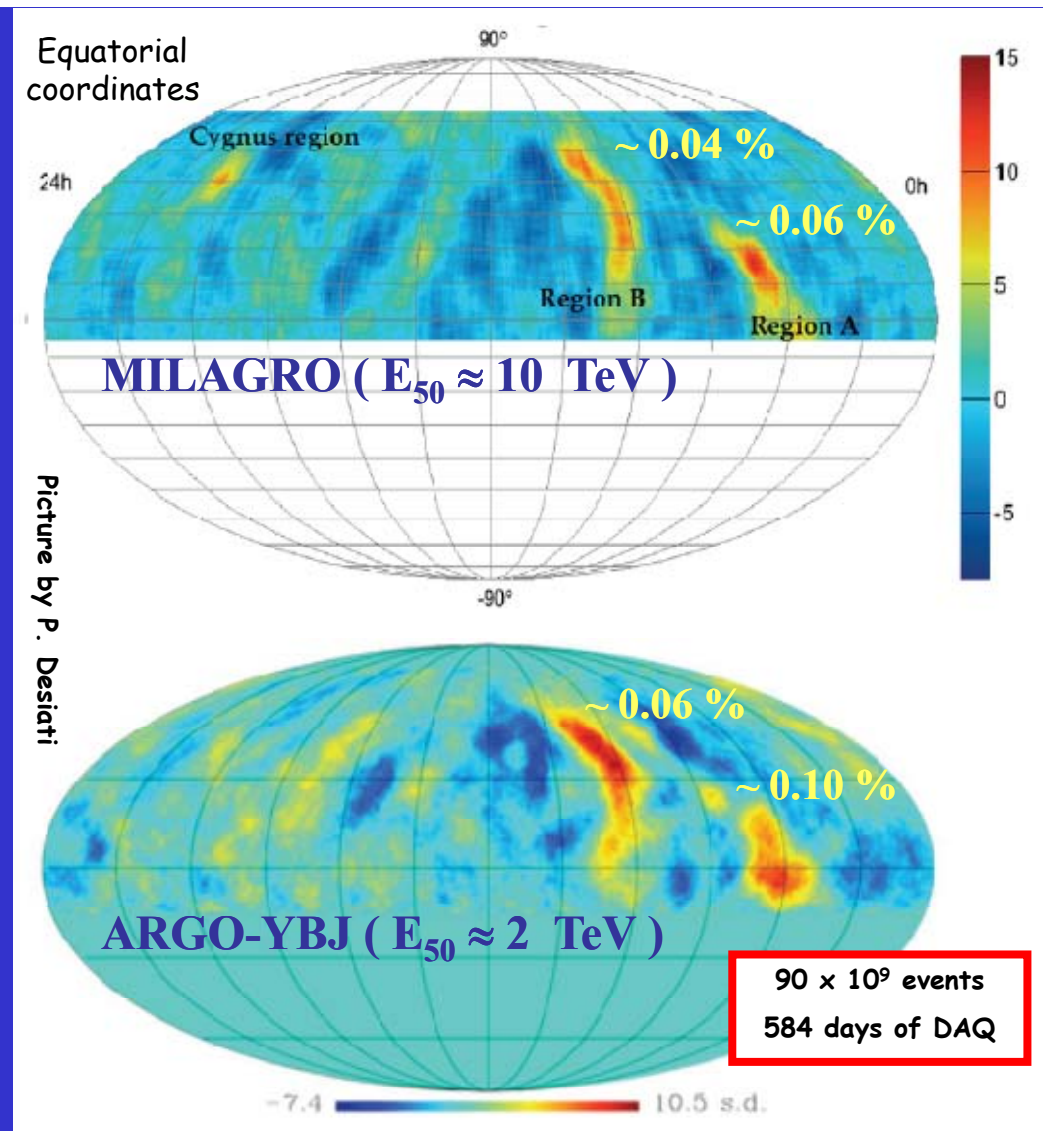
Similar results observed by Tibet AS- γ , Milagro, SuperKamiokande and IceCube at higher energies

Compton-Getting, nearby sources, magnetic field... ?



Medium scale anisotropy of CR

Smaller angular features (medium scale) are visible after removing large angular features (large scale)



These anisotropies must be studied in order to probe the magnetic field in the Earth neighborhood as well as the distribution of CR sources

CR flux

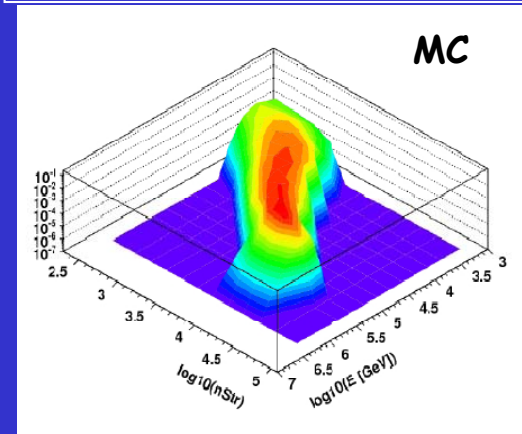


Light-component spectrum of CRs

Measurement of the *light-component* (p+He) spectrum of primary CRs in the range 5–250 TeV via a Bayesian unfolding procedure

- 1) Estimate of $P(N_{\text{HIT}}|E)$ by means of simulation
- 2) Assume $P(E)$
- 3) Apply Bayes theorem $\rightarrow P(E|N_{\text{HIT}})$
- 4) Estimate of $N(E) = N(N_{\text{HIT}}) P(E|N_{\text{HIT}})$
- 5) Calculate new $P(E)$
- 6) Repeat steps 3–5 up to convergence
- 7) Spectrum $N(E)$

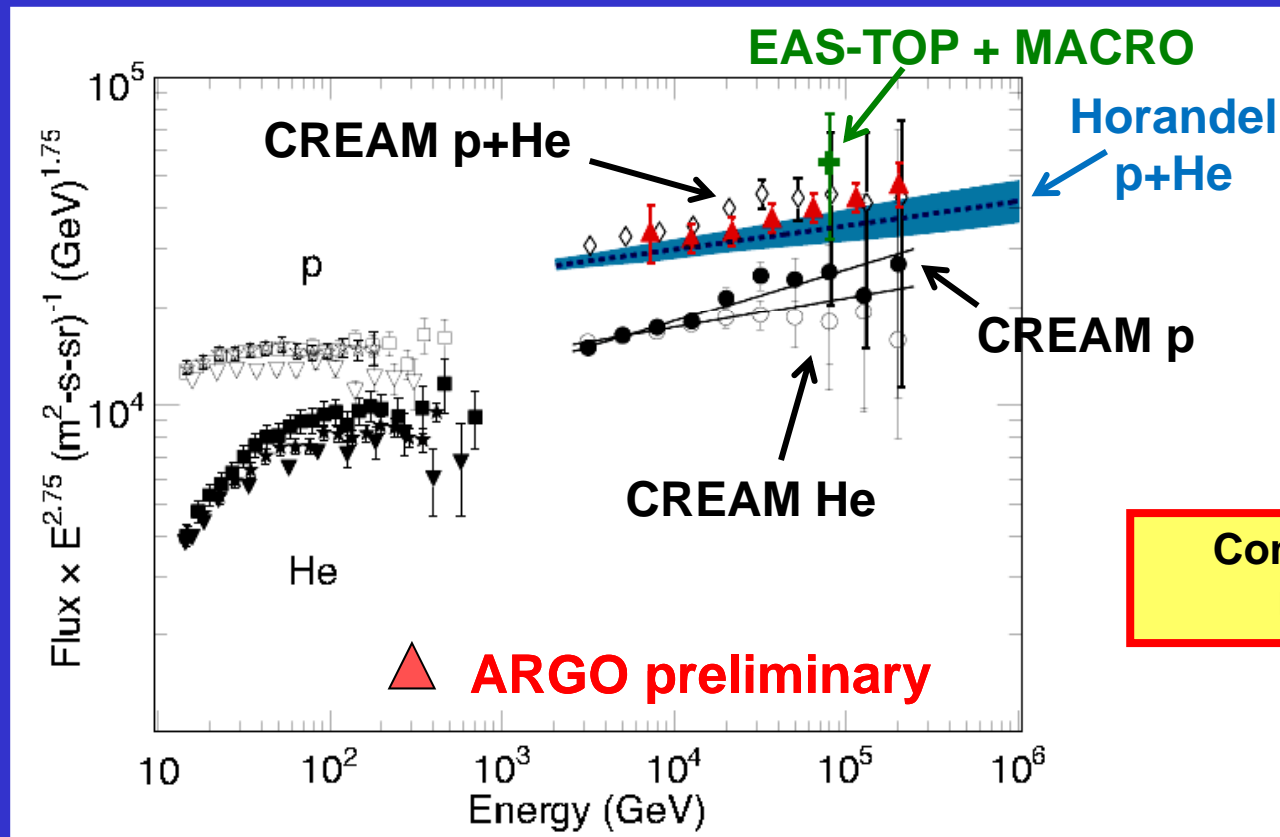
strip multiplicity (N_{HIT})
vs energy



Bayes theorem

$$P(E | N_{\text{HIT}}) = \frac{P(N_{\text{HIT}} | E)P(E)}{P(N_{\text{HIT}})}$$

Light-component spectrum of CRs



Contribution of heavier nuclei is a few %

For the first time direct and ground-based measurements overlap for a wide energy range.

Thus the cross-calibration of the experiments is possible



Proton cross section

Proton-air cross section measurement

Use the shower frequency vs $(\sec \theta - 1)$

$$I(\theta) = I(0) \cdot e^{-\frac{h_0}{\Lambda}(\sec \theta - 1)}$$

for fixed energy and shower age

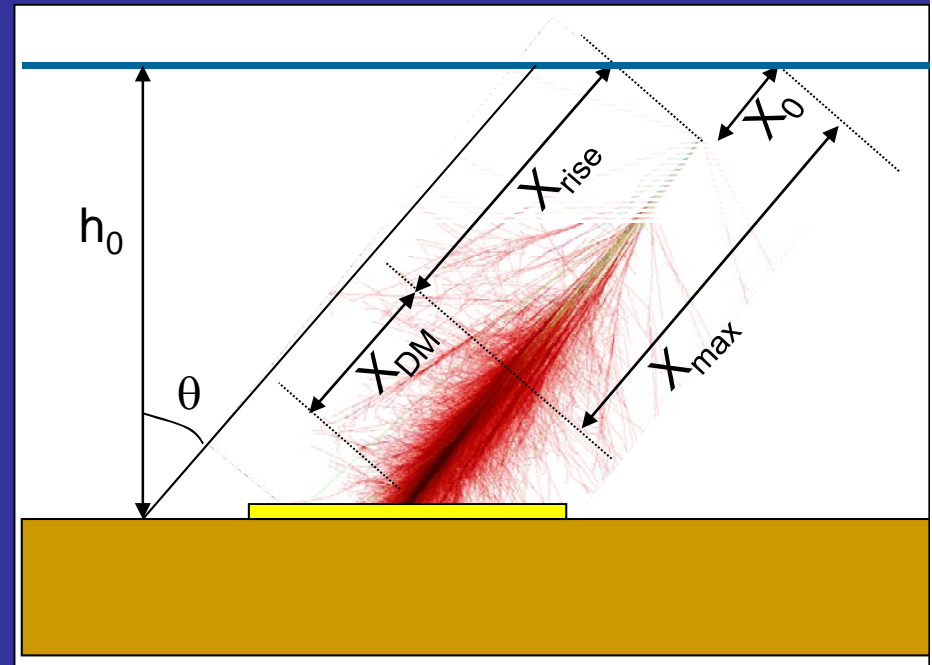
The length Λ is not the p-interaction length mainly because of collision inelasticity, shower fluctuations and detector resolution.

It has been shown that $\Lambda = k \lambda_{\text{int}}$, where k is determined by simulations and depends on:

- **hadronic interactions**
- **detector features and location (atm. depth)**
- **actual set of experimental observables**
- **analysis cuts**
- **energy ...**

Then:

$$\sigma_{\text{p-Air}} \text{ (mb)} = 2.4 \times 10^4 / \lambda_{\text{int}} \text{ (g/cm}^2\text{)}$$



Take care of shower fluctuations

- **Constraint on** $X_{\text{DO}} = X_{\text{det}} - X_0$ or

$$X_{\text{DM}} = X_{\text{det}} - X_{\text{max}}$$

- **Select deep showers**

(large X_{max} , i.e. small X_{DM})

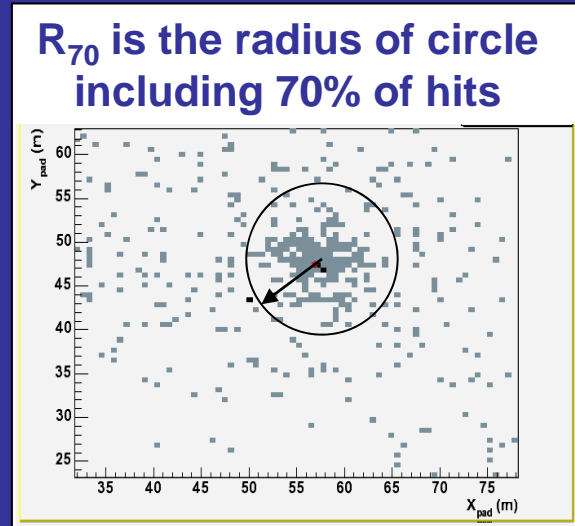
- **Exploit** detector features (space-time pattern) and altitude (depth)

Data selection

➤ Event selection based on:

- (a) “shower size” on detector (N_{strip})
- (b) core reconstructed in a fiducial area ($64 \times 64 \text{ m}^2$)
- (c) constraints on strip density ($> 0.2 \text{ m}^{-2}$ within R_{70})
and shower extension ($R_{70} < 30 \text{ m}$)

N_{strip} is used to get different energy sub-samples

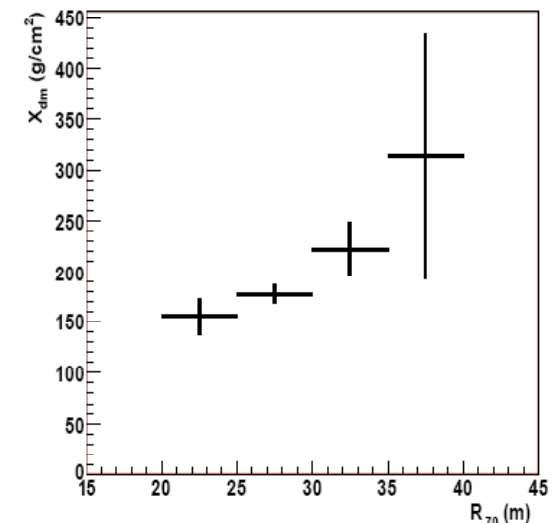
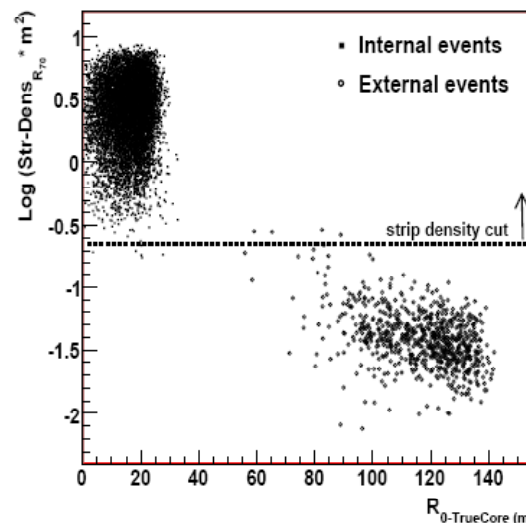


Full Monte Carlo simulation

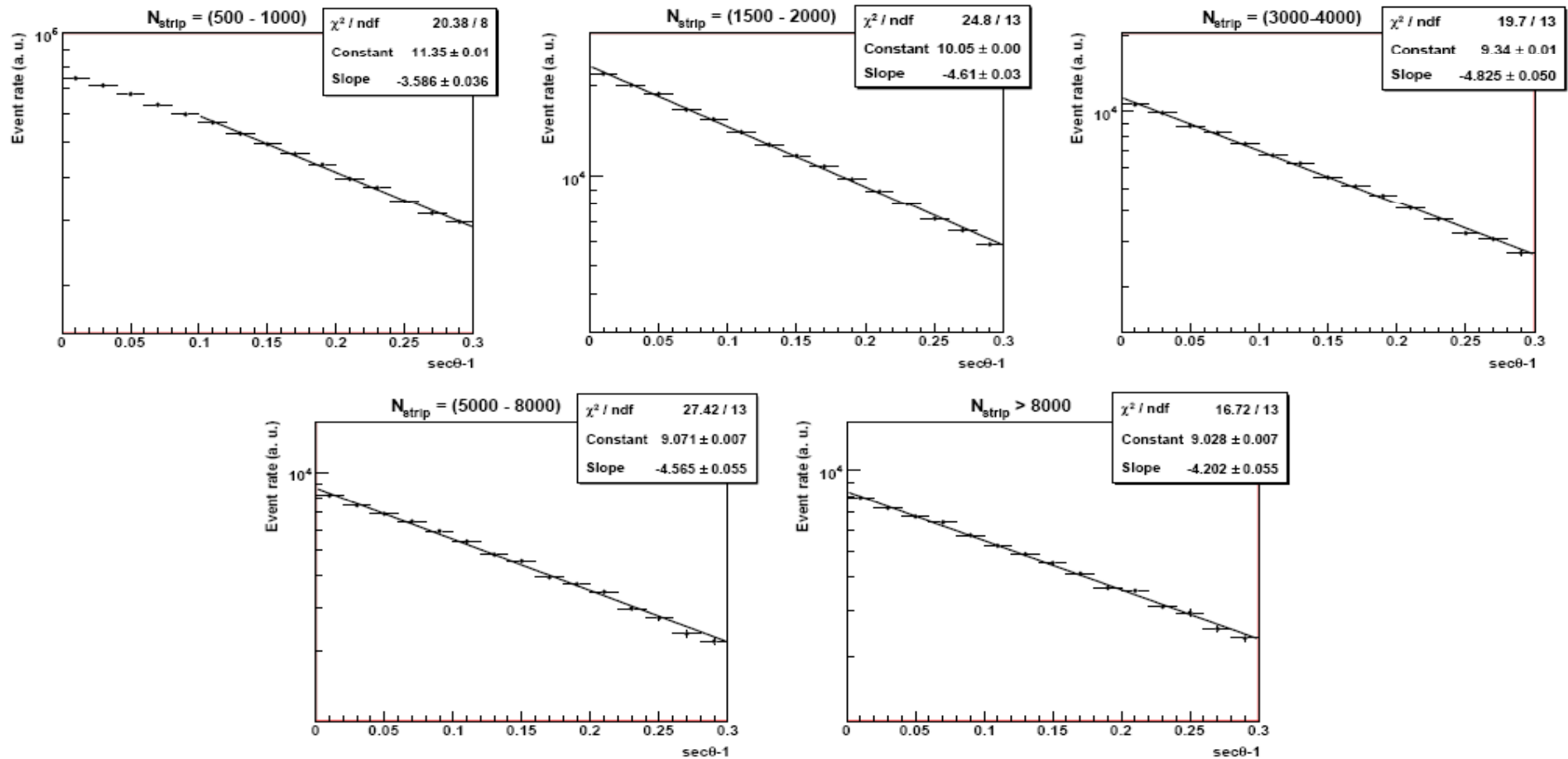
Showers : Corsika

Inter. Models : QGSJET-I
QGSJET-II
SYBILL

Detector : GEANT 3



Experimental data (5 strip multiplicity bins)



$$I(\theta) = I_0 \exp\left[-\frac{h_0}{\Lambda} (\sec\theta - 1)\right]$$

$$I(\theta) = I_0 \exp \left[-\frac{h_0}{\Lambda} (\sec \theta - 1) \right]$$

$$\lambda_{\text{INT}} = \Lambda / k$$

$$\sigma_{p\text{-Air}} [\text{mb}] = 2.4 \times 10^4 / \lambda_{\text{INT}} [\text{g} / \text{cm}^2]$$



ΔN_{strip}	$\text{Log}(E/\text{eV})$	$k_{\text{QGSJET-I}}$	$k_{\text{QGSJET-II.03}}$	$k_{\text{SIBYLL-2.1}}$	k
500 ÷ 1000	12.6 ± 0.3	1.98 ± 0.06 ± 0.05	1.84 ± 0.14 ± 0.05	1.87 ± 0.08 ± 0.04	1.93 ± 0.05 ± 0.06
1500 ÷ 2000	13.0 ± 0.2	1.59 ± 0.03 ± 0.04	1.75 ± 0.12 ± 0.04	1.76 ± 0.06 ± 0.04	1.63 ± 0.03 ± 0.08
3000 ÷ 4000	13.3 ± 0.2	1.69 ± 0.05 ± 0.03	1.63 ± 0.13 ± 0.03	1.72 ± 0.05 ± 0.03	1.70 ± 0.03 ± 0.04
5000 ÷ 8000	13.6 ± 0.2	1.74 ± 0.05 ± 0.03	1.97 ± 0.17 ± 0.04	1.91 ± 0.05 ± 0.03	1.84 ± 0.03 ± 0.10
> 8000	13.9 ± 0.3	2.04 ± 0.06 ± 0.05	2.23 ± 0.19 ± 0.05	2.01 ± 0.05 ± 0.05	2.03 ± 0.04 ± 0.10

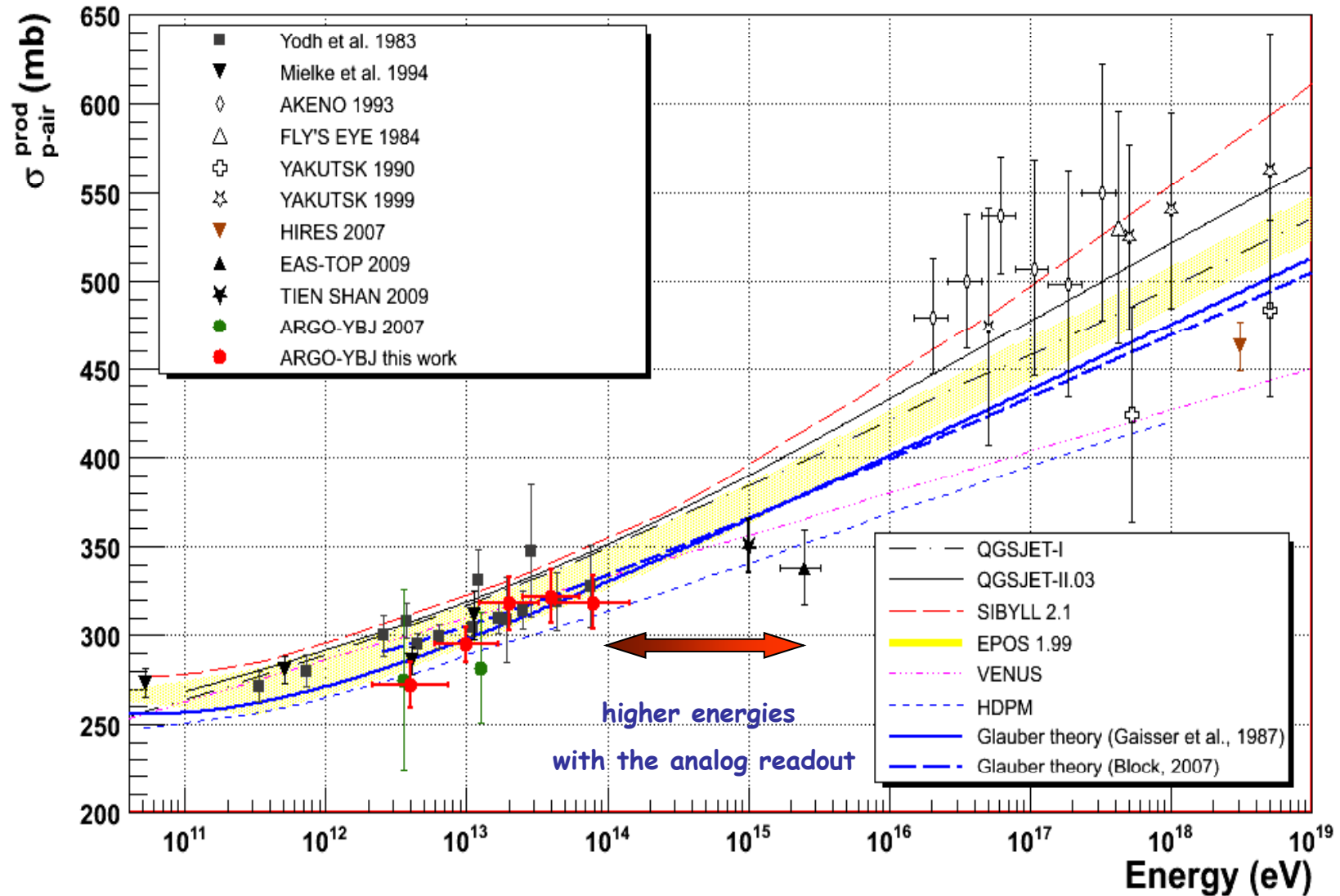
Correction factor for heavier primaries

Glauber theory applied
(model differences in the sys errors)

ΔN_{strip}	η	$\sigma_{p\text{-air}}$ (mb)	$\sigma_{p\text{-p}}$ (mb)
500 ÷ 1000	1.00 ± 0.04 ± 0.01	272 ± 13 ± 9	43 ± 3 ± 5
1500 ÷ 2000	1.00 ± 0.03 ± 0.01	295 ± 10 ± 14	48 ± 3 ± 6
3000 ÷ 4000	0.99 ± 0.04 ± 0.01	318 ± 15 ± 8	54 ± 4 ± 6
5000 ÷ 8000	0.98 ± 0.04 ± 0.03	322 ± 15 ± 20	56 ± 4 ± 7
> 8000	0.95 ± 0.04 ± 0.04	318 ± 15 ± 21	54 ± 4 ± 8

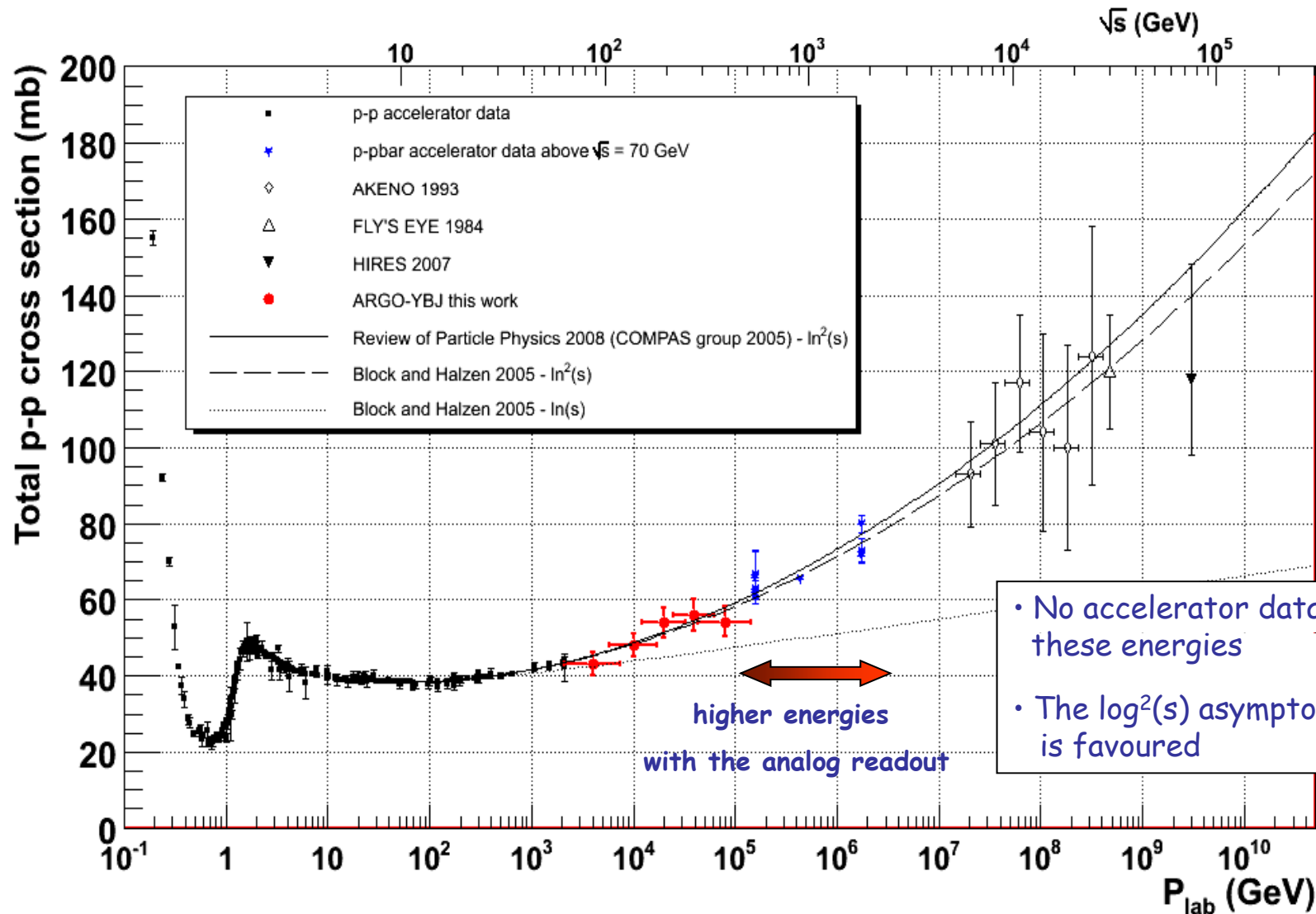
Proton-air cross section

Phys. Review D 80 (2009) 092004



Total p-p cross section

Phys. Review D 80 (2009) 092004



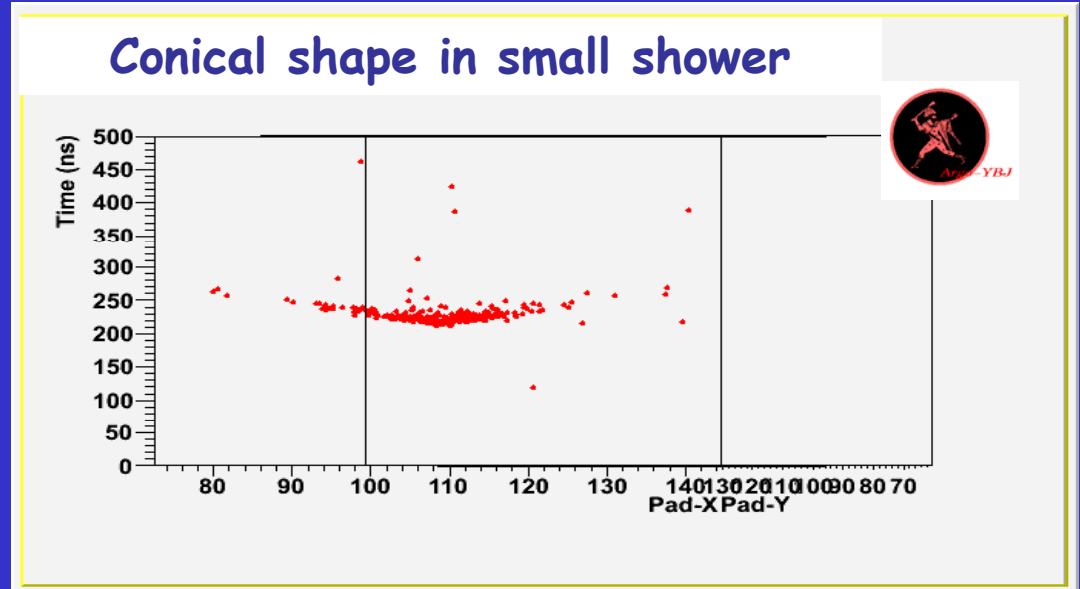
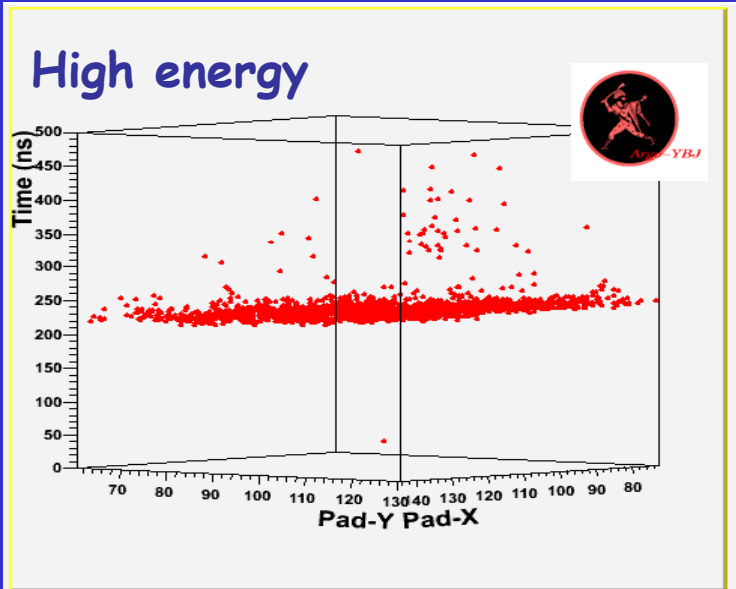
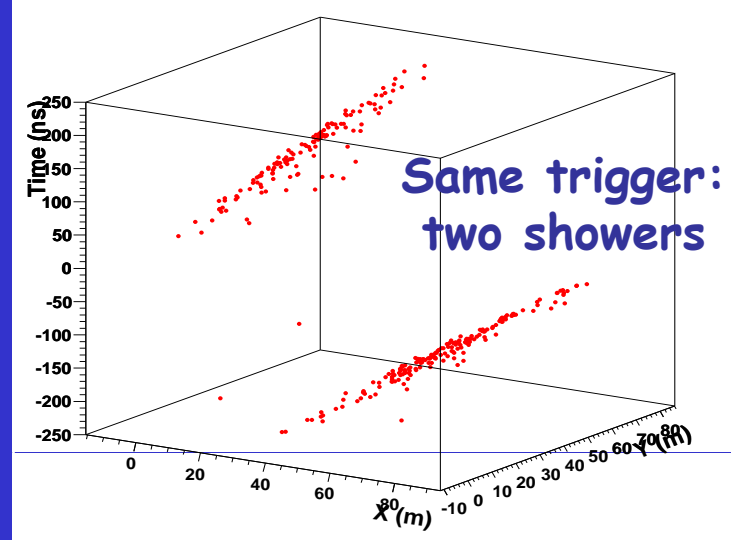
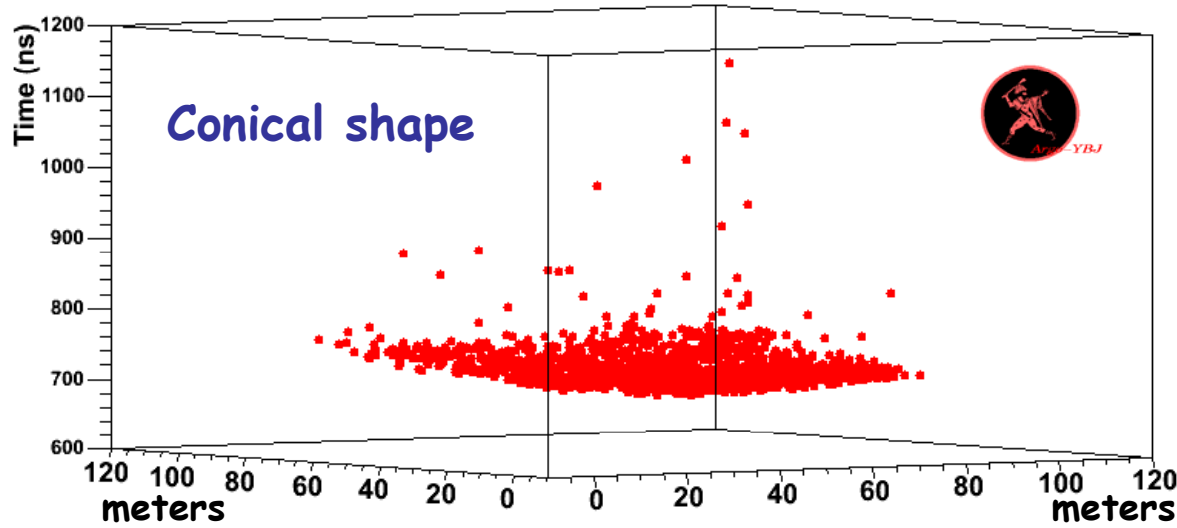
Shower features



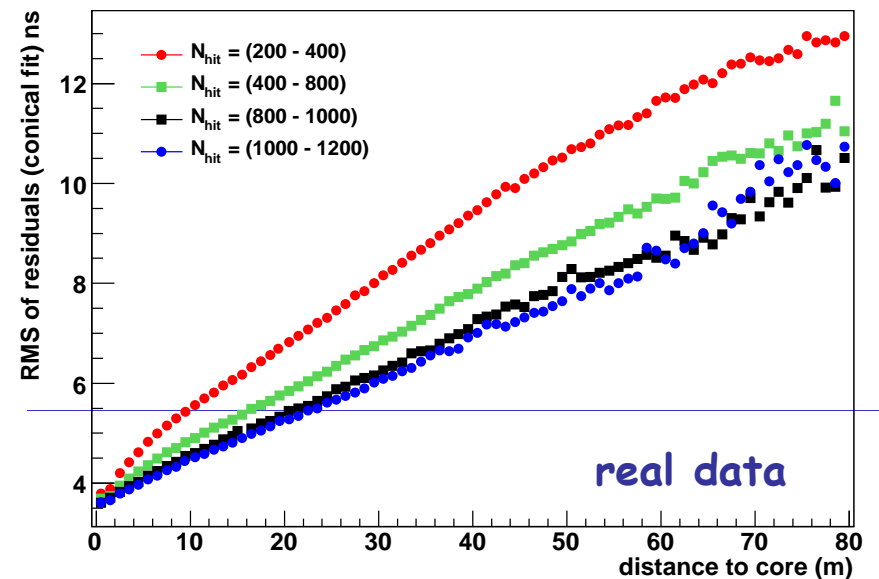
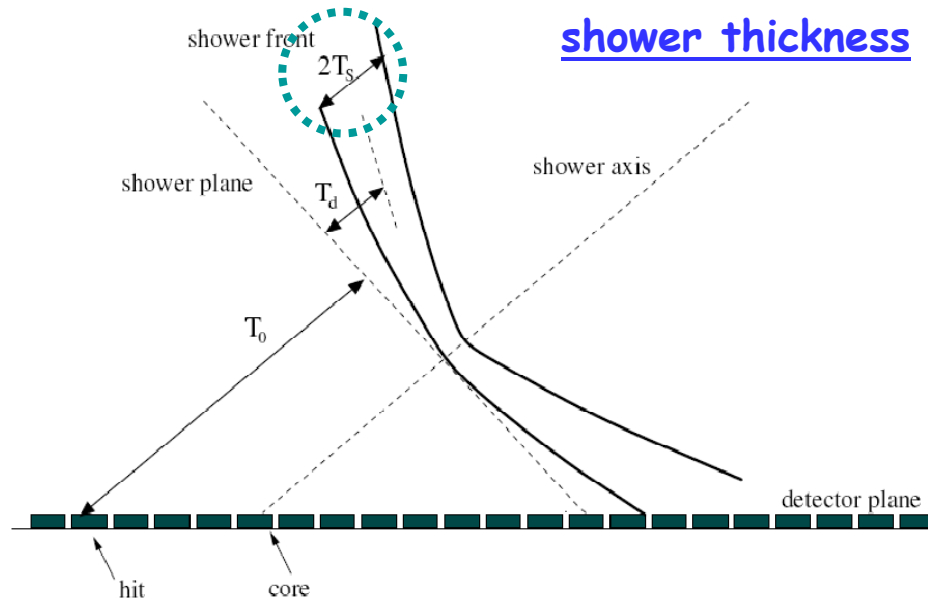
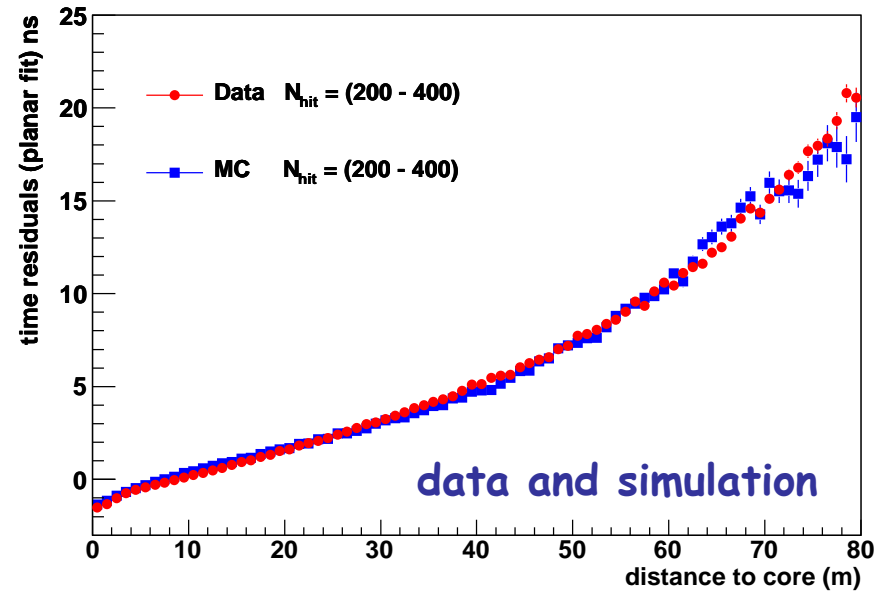
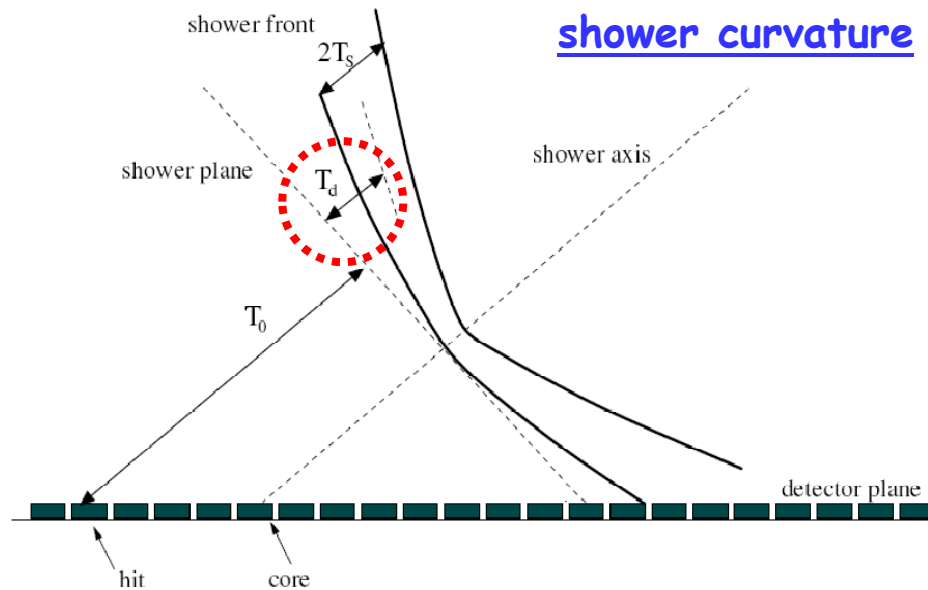
The number of pixels, the time resolution and the full coverage allow to "see" the showers with unprecedented details

ARGO-130

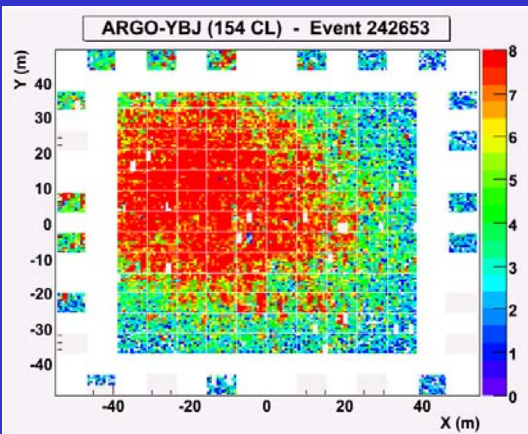
Event 394
Mean x 30.02
Mean y 30.14



Studies on the shower time structure

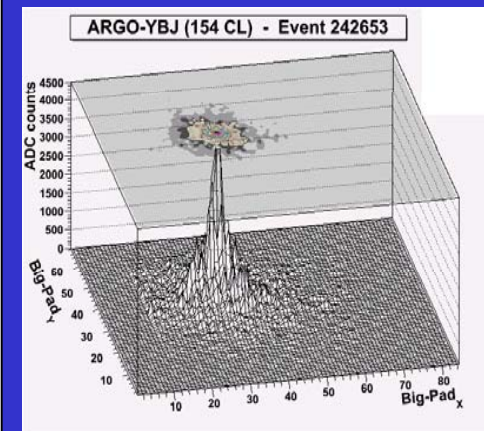
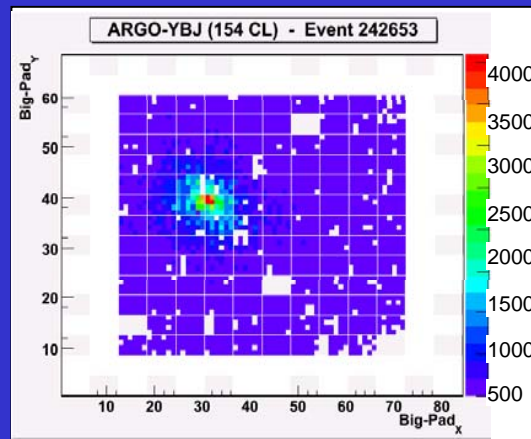


Improvements with the analog readout (real events)

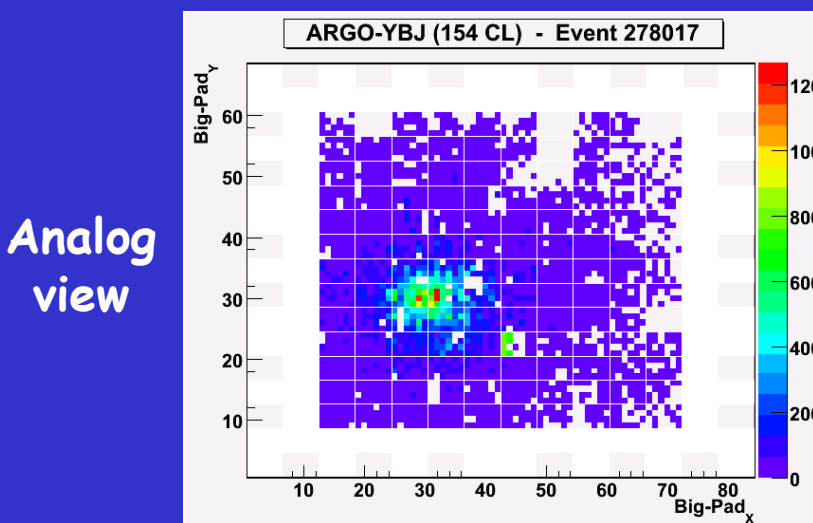


Digital view

Analog view

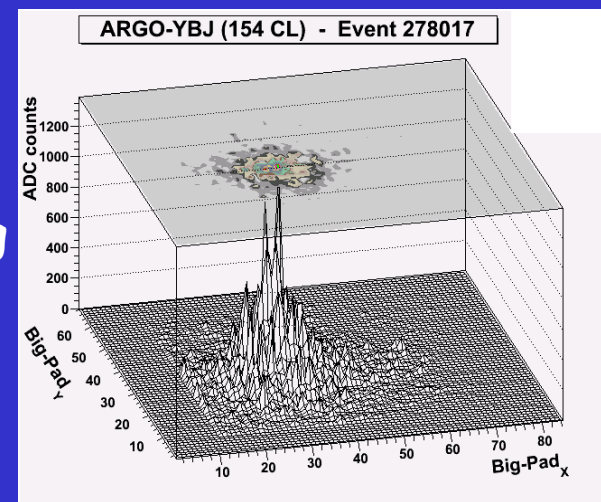


Multicore real event

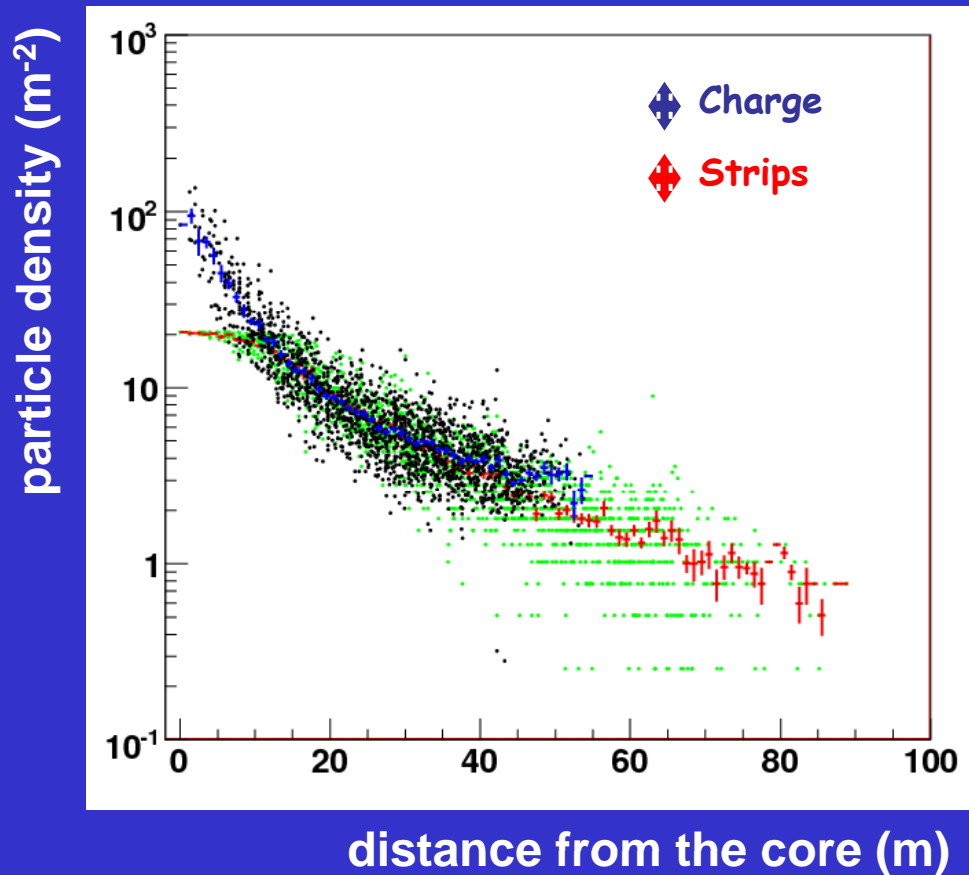


Analog view

Analog view



Lateral Distribution Function



Unprecedented

With the analog data the LDF can be studied without saturation near the core

- ✓ Better resolution on X_{DM} and lower systematics on the cross section measurement
- ✓ Better energy estimate and shower reconstruction

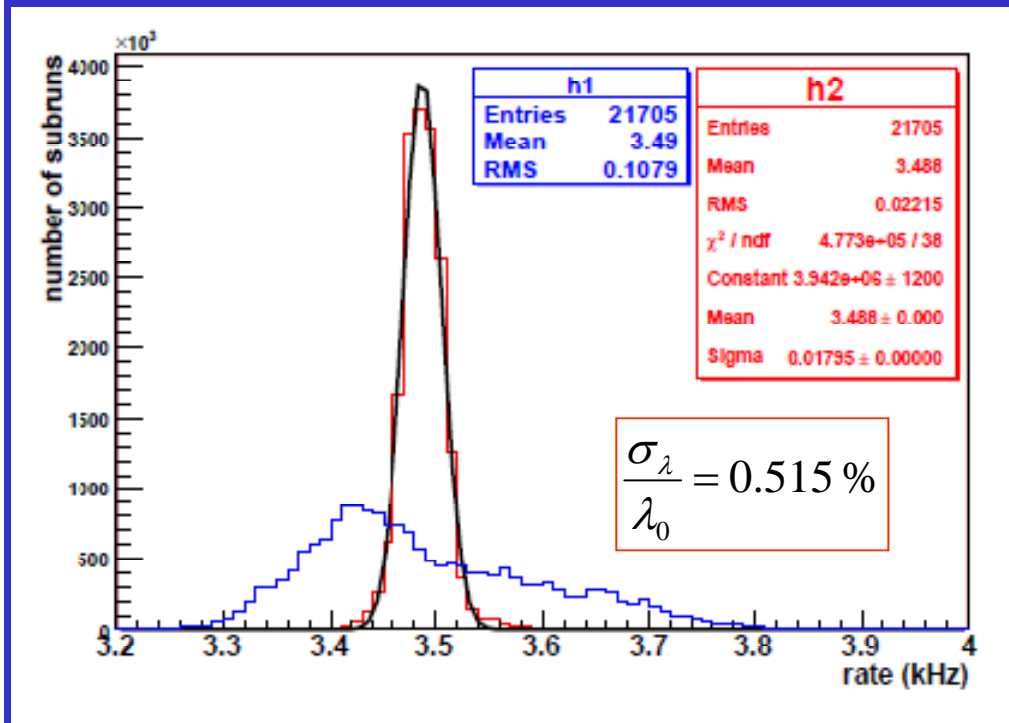
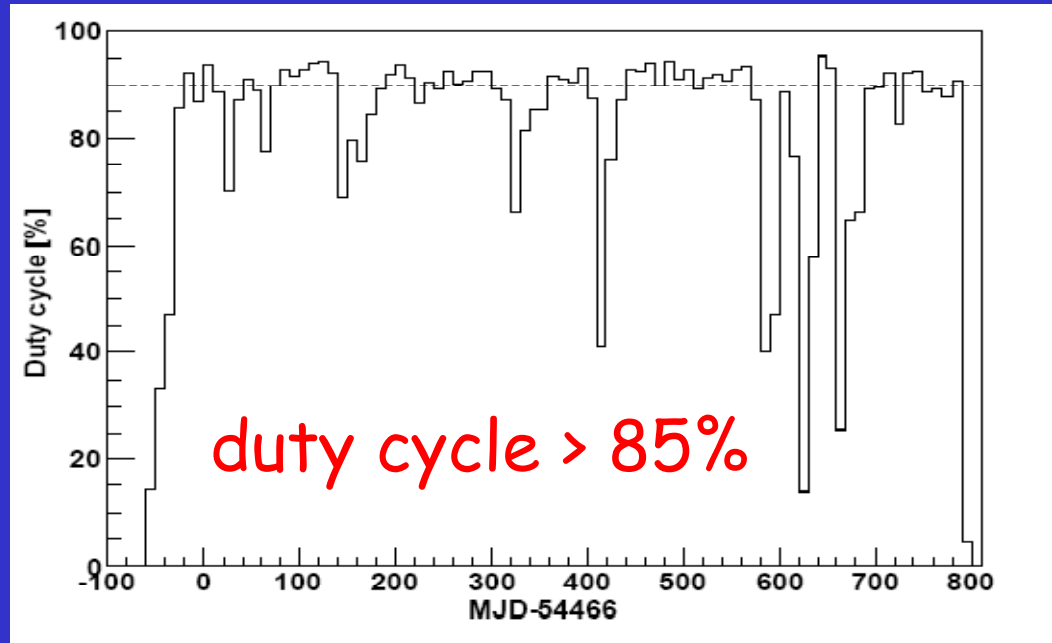
Looking for observable quantities
to make crucial test
on hadronic interaction models

Conclusions

- ✓ **ARGO-YBJ detector (central carpet + guard ring)**
is taking data since November 2007
- ✓ **Sky survey in VHE gamma band is going on**
- ✓ **Many results on CR physics**
 - p-air and p-p cross section
 - large and medium scale anisotropies
 - Moon (and Sun) shadow
 - limit on anti-proton flux
 - spectrum of CR light-component (Bayesian method)
- ✓ **Improvement of the CR studies (new analyses, analog read-out)**
 - p-p cross section up to PeV
 - standard estimate of the CR flux
 - study on the lateral distribution very close to the core
 - test on hadronic interactions looking at shower time-structure, lateral distribution and at multi-core events

BUFFER SLIDES

Detector Stability

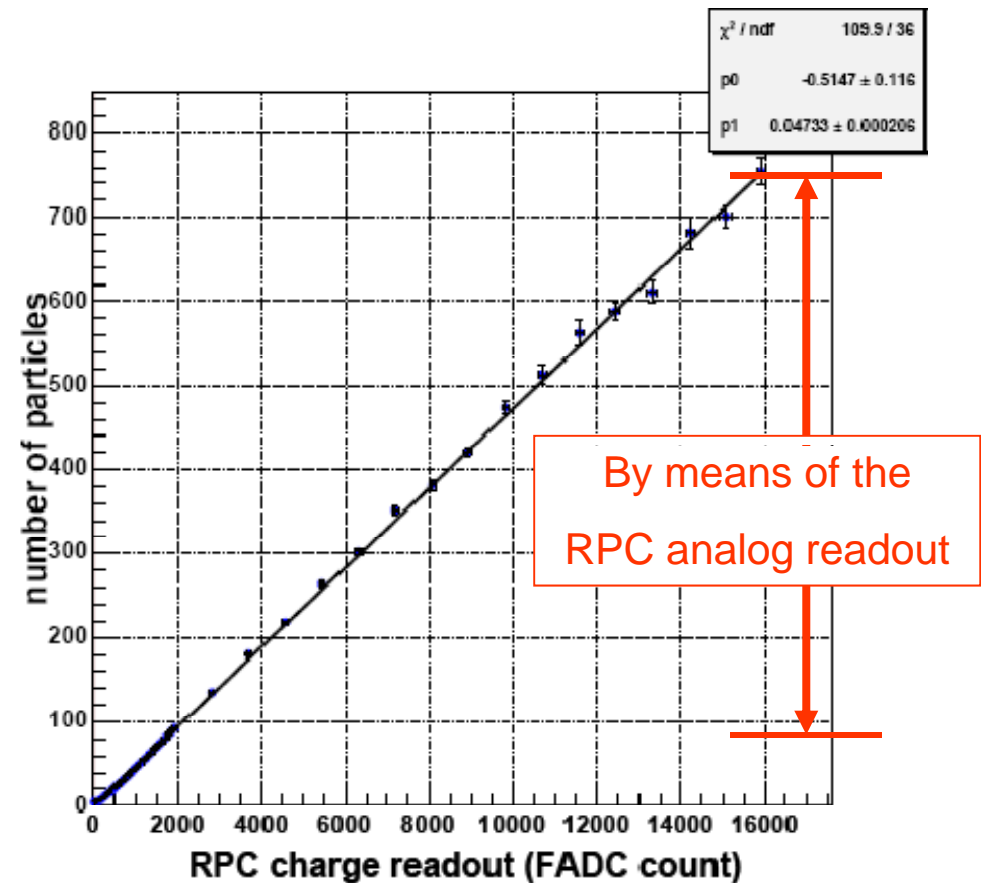
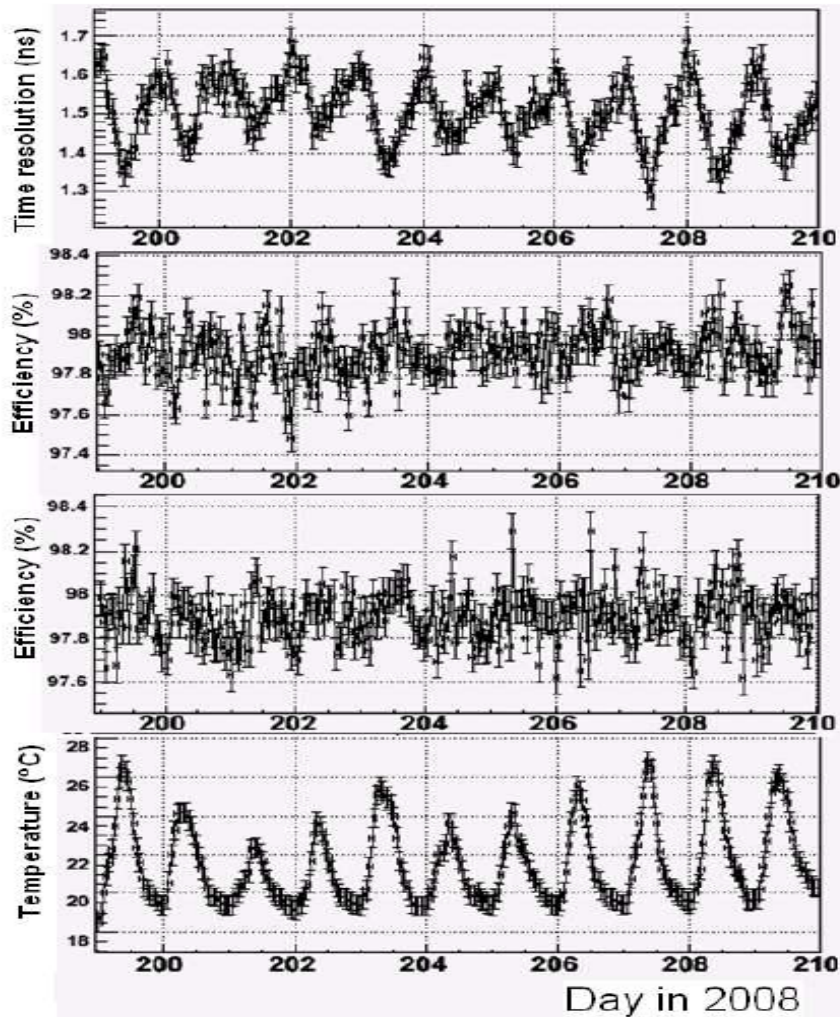


event rate variations

$\pm 0.5\%$

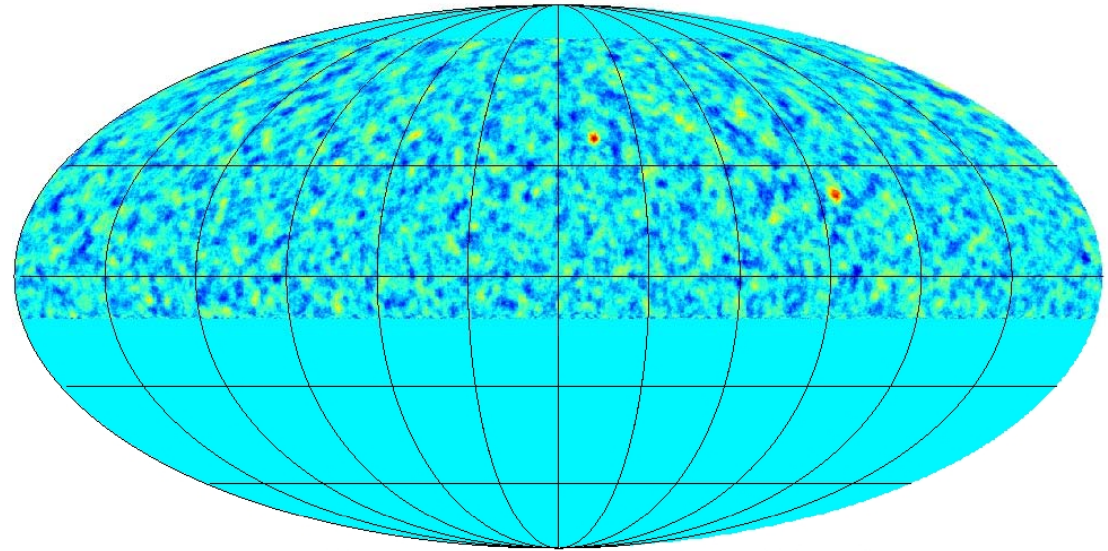
after correction for
barometric effects

RPC performance and linearity range



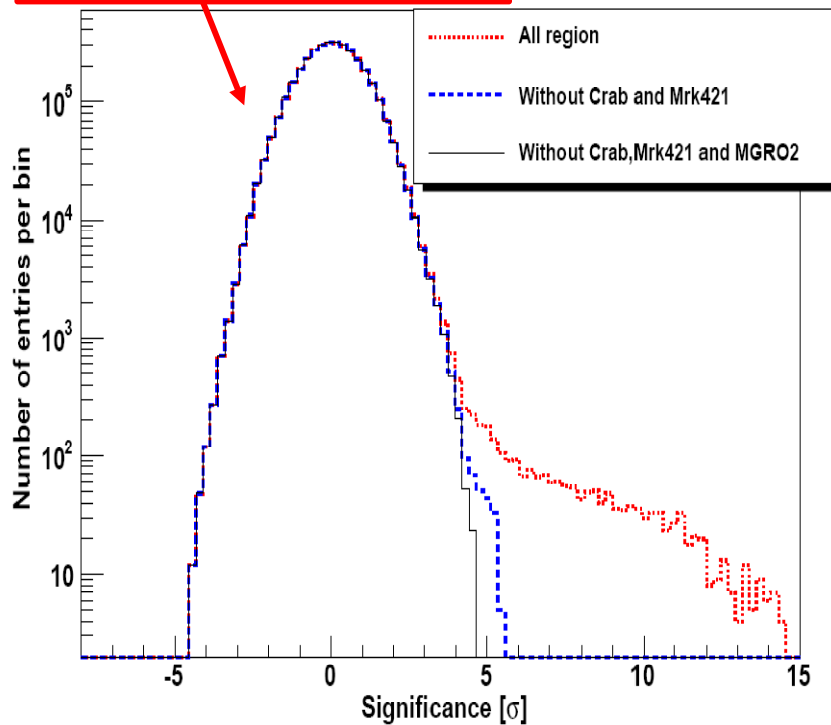
γ -astronomy

Many results on long term variabilities correlation with X-band spectra ...



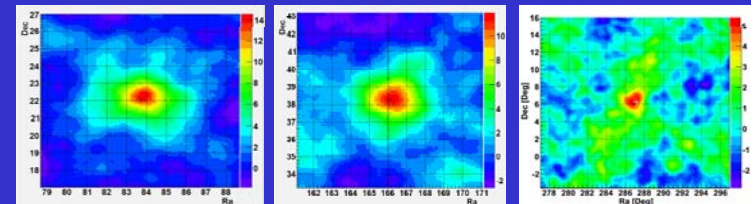
Mean = $(-9.3 \pm 2.1) \times 10^{-3}$
 Sigma = 1.008 ± 0.002

$N_{\text{HIT}} > 40 \rightarrow$ Gamma median energy $\approx 0.6-2$ TeV

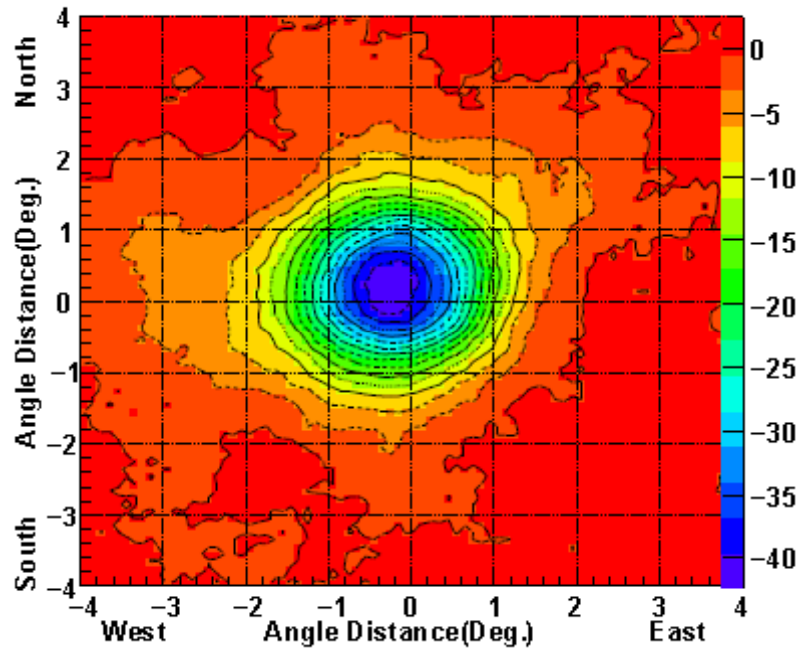


~ 800 day data \rightarrow 3 sources with significance $> 5 \sigma$

Crab	14 σ
Mrk 421	12 σ
MGRO J1908+06	6 σ

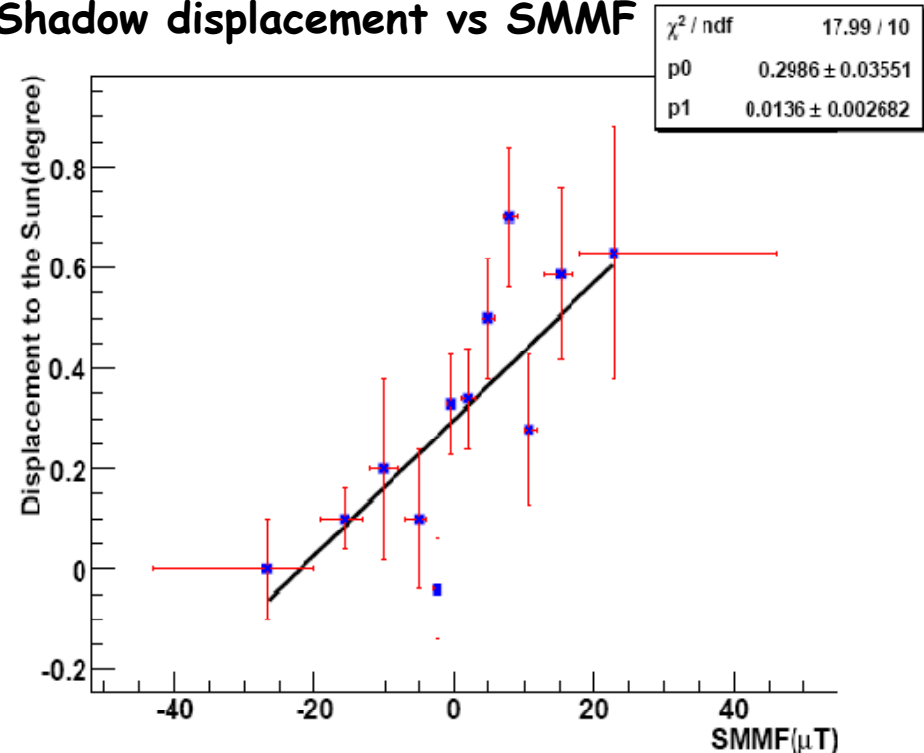


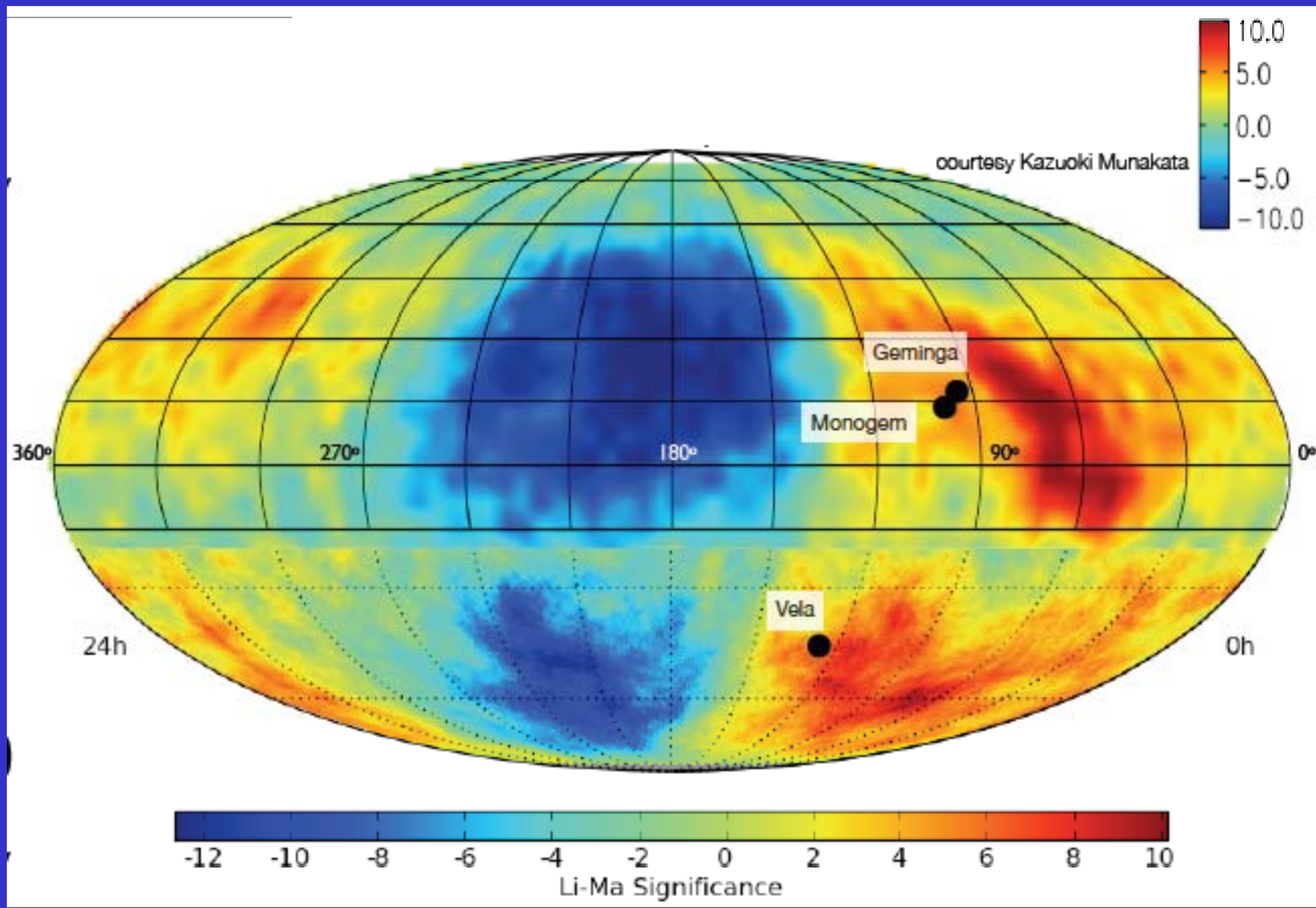
The Sun shadow to explore the solar magnetic field



The displacement of the Sun shadow is a good measurement of the IMF, especially in this particular quiet phase (23th - 24th cycle)

Shadow displacement vs SMMF





Medium scale anisotropy of CR

Smaller angular features (medium scale) are visible after removing large angular features (large scale)

Possible explanations:

Heliospheric tail

Karapetyan, *Astrop. Phys.*
33 (2010) 146

Lazarian & Desiati, *ApJ*.
722 (2010) 188

IS magnetic field turbulence

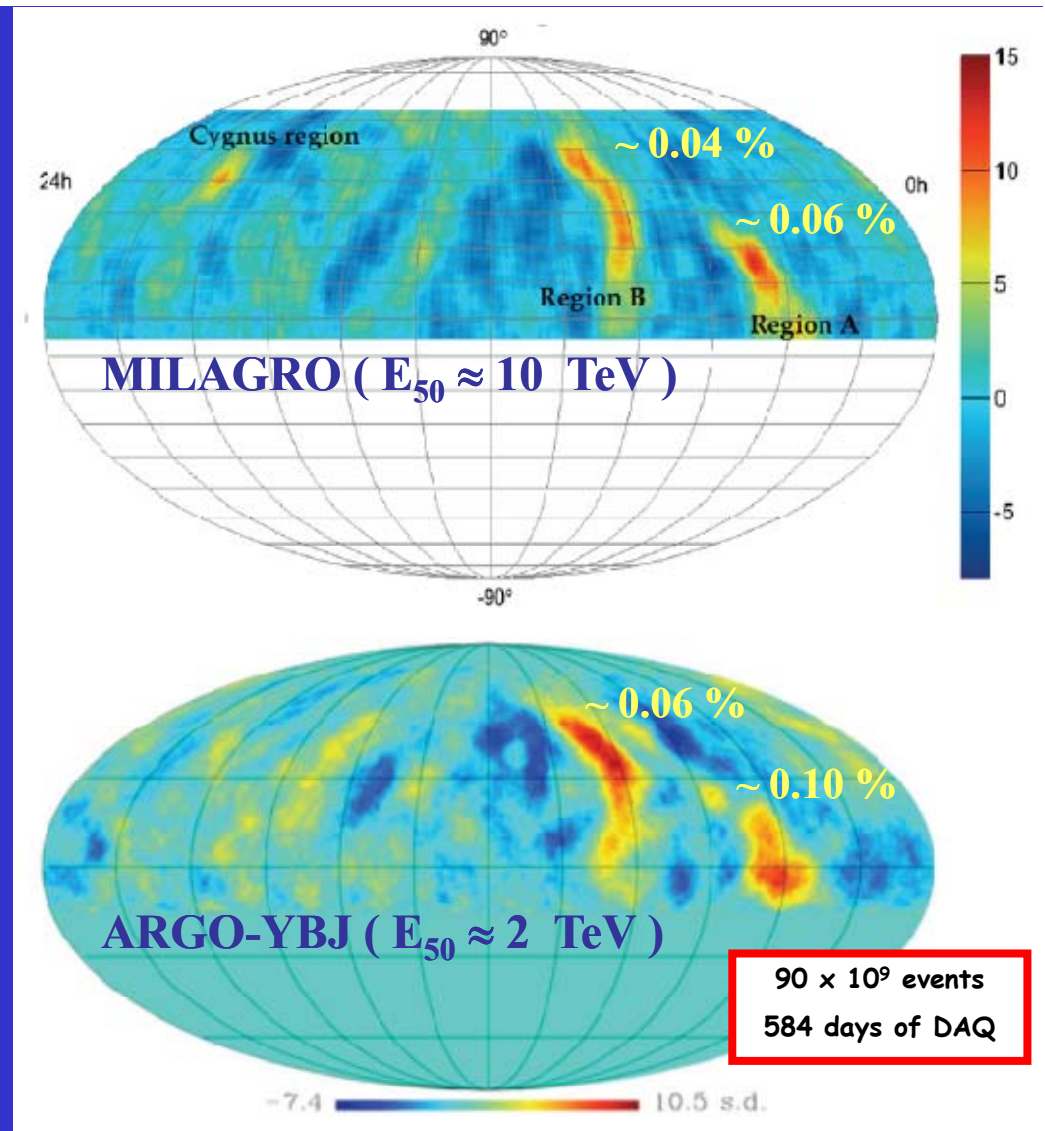
Malkov et al, arXiv:1005.1312

Galactic CR accelerator (Geminga ...)

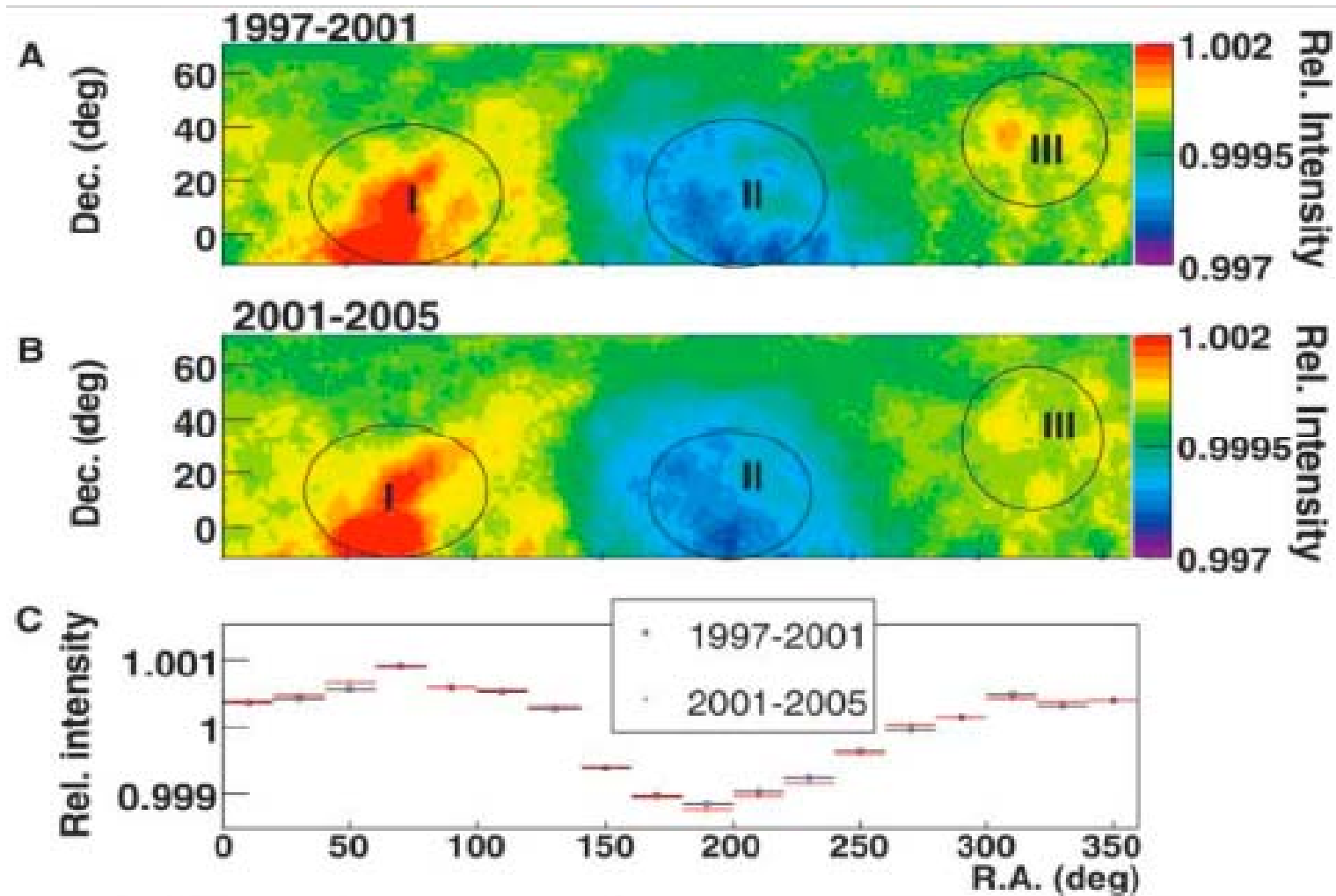
Salvati & Sacco, *A&A* 485 (2008) 527

Drury & Aharonian, *Astrop. Phys.* 29 (2008) 420

Salvati, *A&A* 513 (2010) A28



Tibet $AS\gamma$

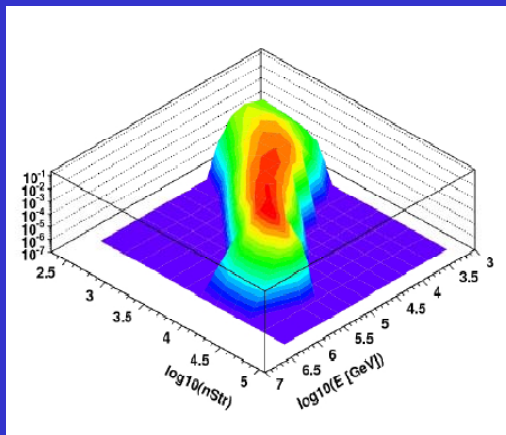


M. Amenomori et.al. Science, 2006

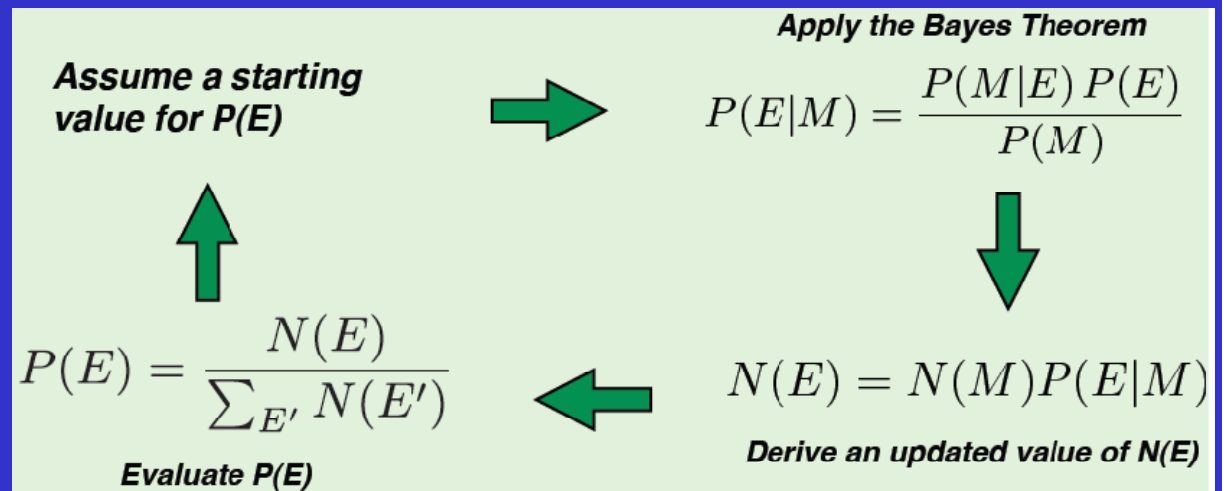
Light-component spectrum of CRs

Measurement of the *light-component* (p+He) spectrum of primary CRs in the range 5–250 TeV via a Bayesian unfolding procedure

strip multiplicity (M)
vs energy

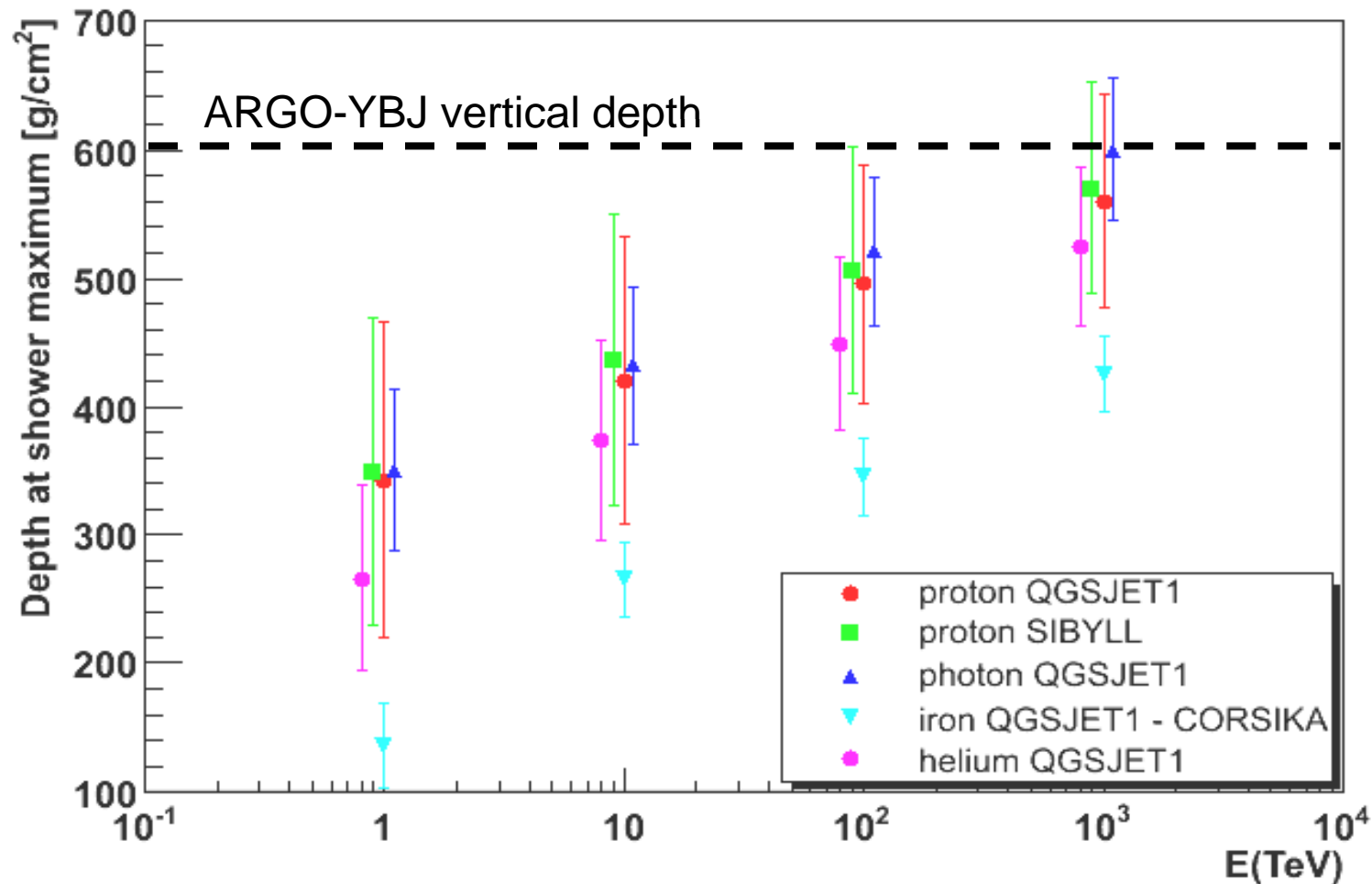


- 1) Estimate of $P(M|E)$ by means of simulation
- 2) Iterative procedure



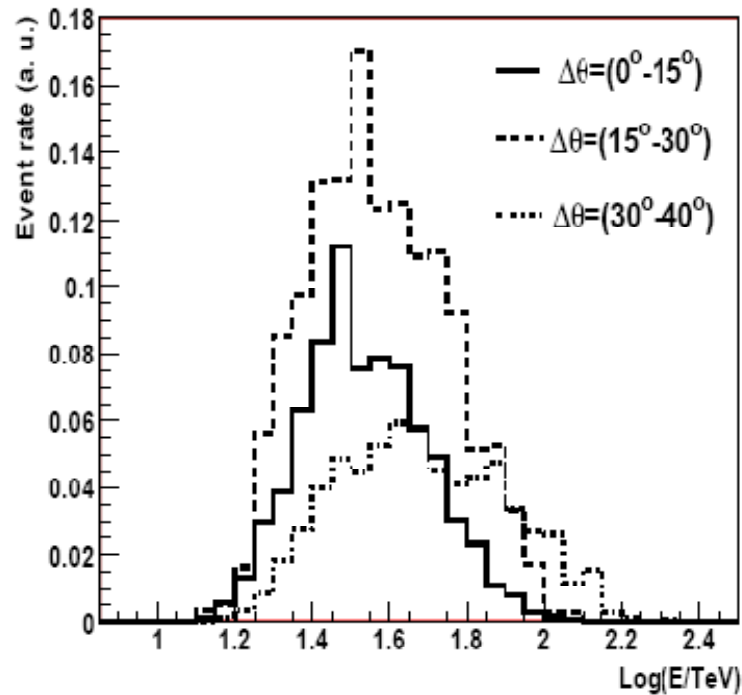
3) Spectrum $N(E) = N(M) P(E|M)$

The position of the shower maximum (and its rms)

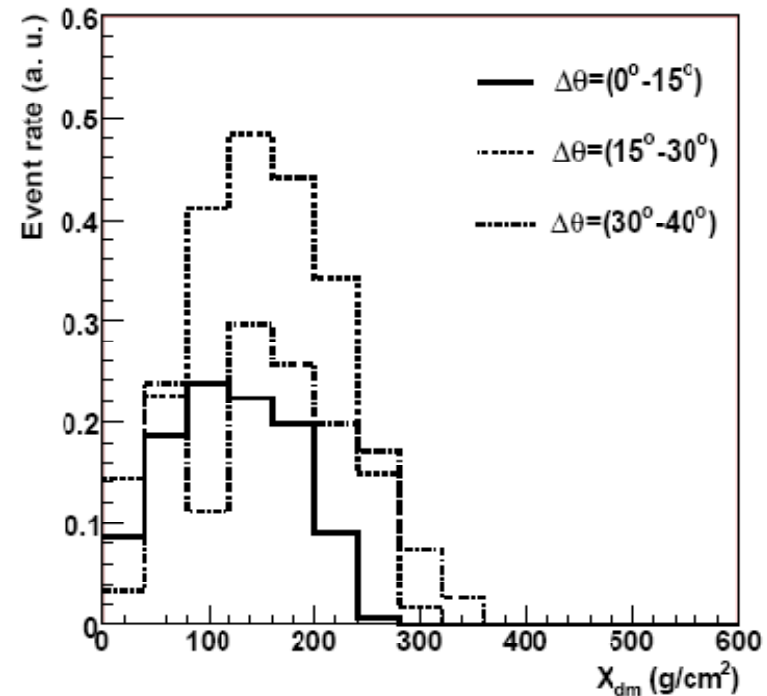


Cuts in-dependence on the zenith angle

Energy



$X_{\text{det}} - X_{\text{max}}$



No significant zenith angle dependence below 30 degrees.

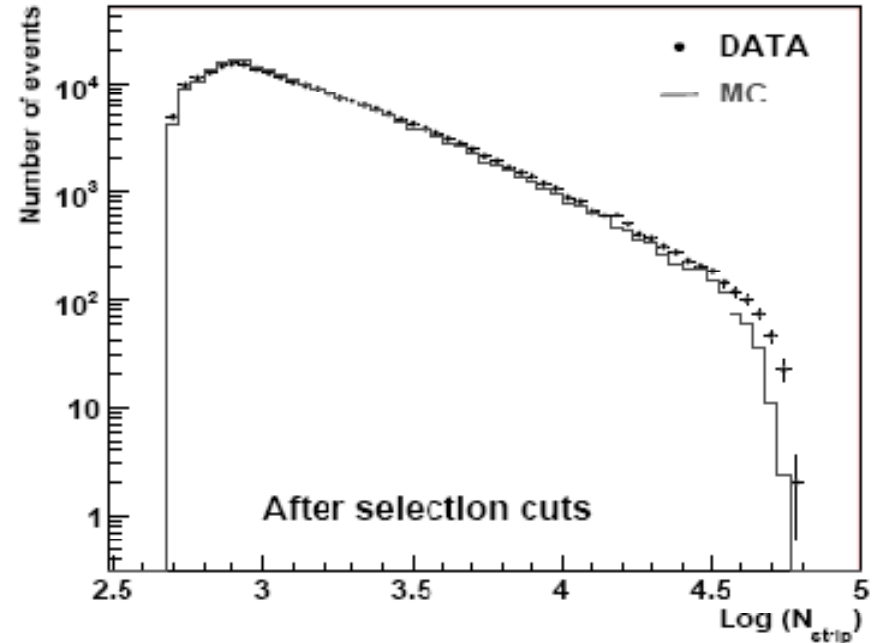
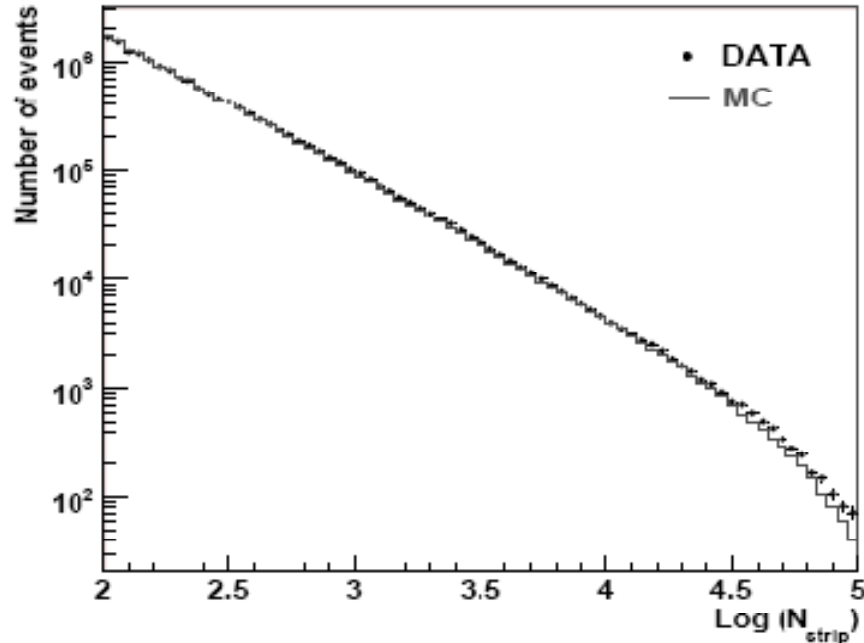
A slight shift might be seen above 40 degrees.

In this analysis we stop at 40 degrees

MC vs DATA

The distributions of the measured quantities before and after the analysis cuts are in good agreement with the simulation

The effects of the analysis cuts are consistent (at each step) with the MC estimate



Heavy primaries contribution

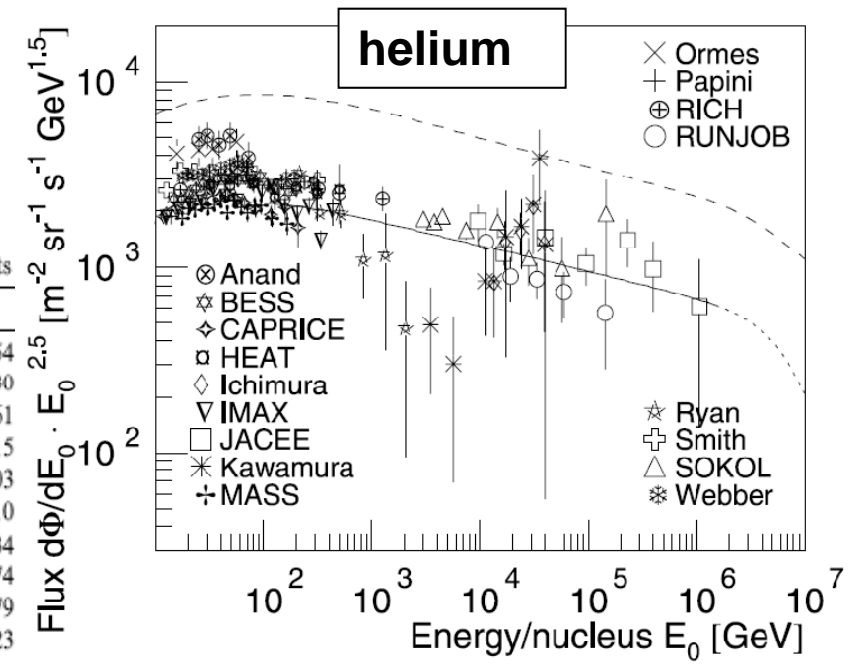
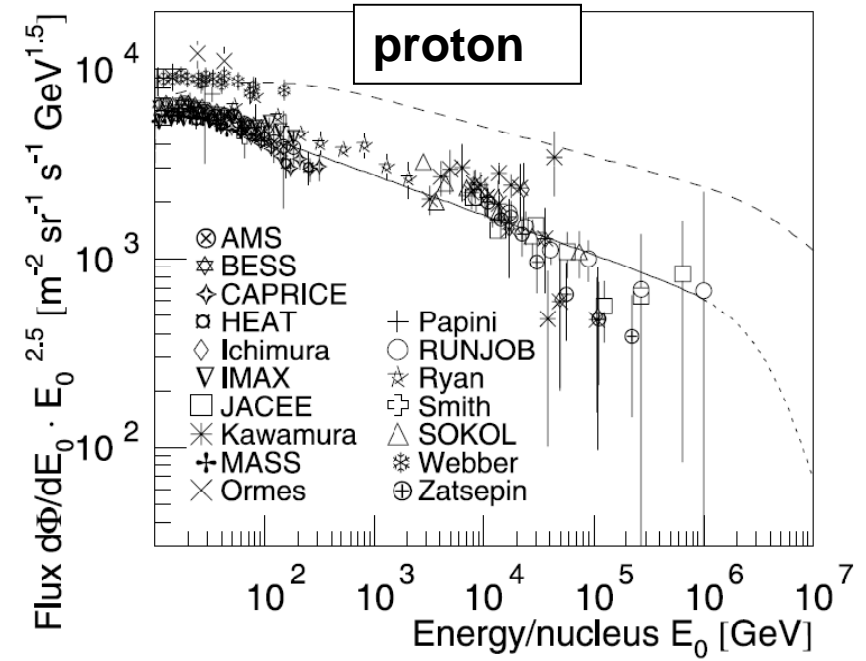
Hoerandel AP 19 (2003) 193 taken as reference.

JACEE and RUNJOB for the evaluation of systematic error

$$\frac{dN}{dE} = \Phi(E) = \Phi_Z^0 \cdot \left(\frac{E}{TeV} \right)^{-\gamma_Z}$$

Table 1
Absolute flux Φ_Z^0 ((m² sr s TeV)⁻¹) at $E_0 = 1$ TeV/nucleus and spectral index γ_Z of cosmic-ray elements

Z		Φ_Z^0	$-\gamma_Z$	Z		Φ_Z^0
1 ^a	H	8.73×10^{-2}	2.71	47 ^c	Ag	4.54
2 ^a	He	5.71×10^{-2}	2.64	48 ^c	Cd	6.30
3 ^b	Li	2.08×10^{-3}	2.54	49 ^c	In	1.61
4 ^b	Be	4.74×10^{-4}	2.75	50 ^c	Sn	7.15
5 ^b	B	8.95×10^{-4}	2.95	51 ^c	Sb	2.03
6 ^b	C	1.06×10^{-2}	2.66	52 ^c	Te	9.10
7 ^b	N	2.35×10^{-3}	2.72	53 ^c	I	1.34
8 ^b	O	1.57×10^{-2}	2.68	54 ^c	Xe	5.74
9 ^b	F	3.28×10^{-4}	2.69	55 ^c	Cs	2.79
10 ^b	Ne	4.60×10^{-3}	2.64	56 ^c	Ba	1.23



Systematics

Effect of the atmospheric pressure at the level of 1 %

$$h_0^{MC} / h_0^{real} = 0.988 \pm 0.007$$

Heavy primaries contribution

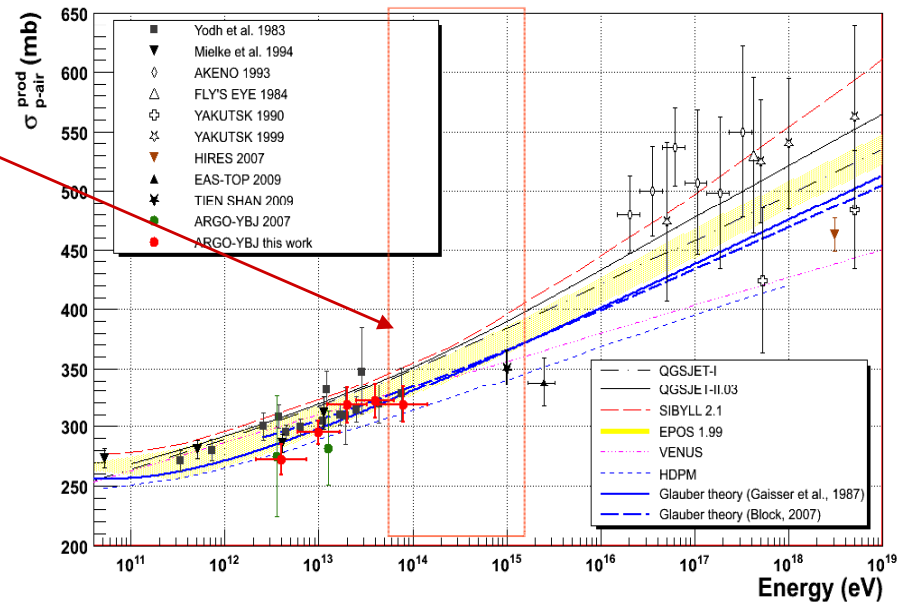
Horandel, Astr. Phys. 19 (2003) 193 as reference
JACEE and RUNJOB to estimate the errors

Interaction models

The spread among the models (QGSJET-I, QGSJET-II.03, SIBYLL 2.1) has been used in order to have a conservative estimate of the associated uncertainties

Next steps in the cross section analysis

- Use the analog RPC charge readout to extend the Energy range
- Better estimate of systematics



Improvements are expected from:

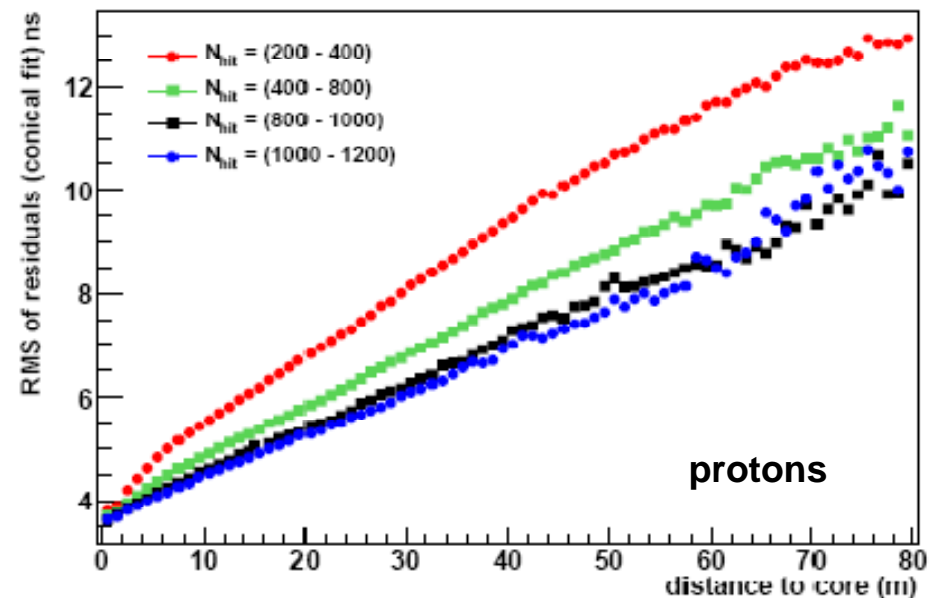
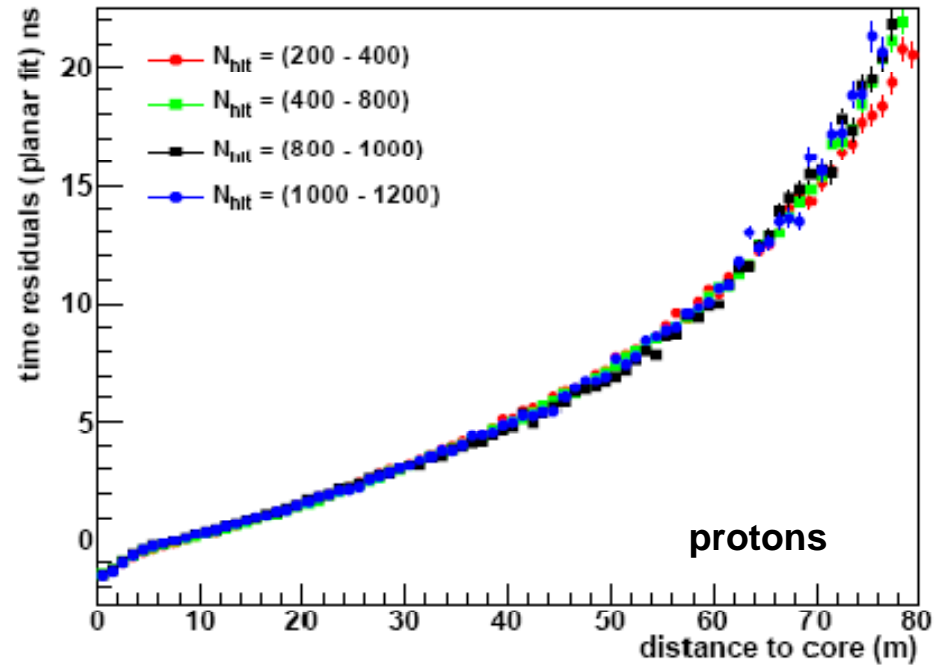
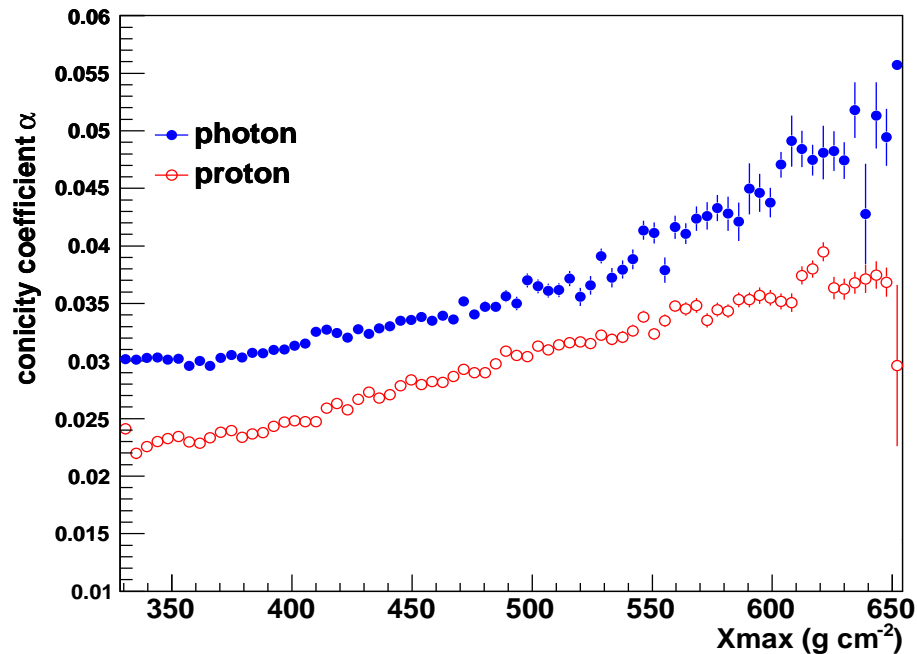
- (a) More detailed informations on the shower time structure, longitudinal development and lateral density profile (LDF)
- (b) Better constraints on shower X_{max} (\rightarrow lower systematics)

... also given by the RPC charge information

Shower front time structure

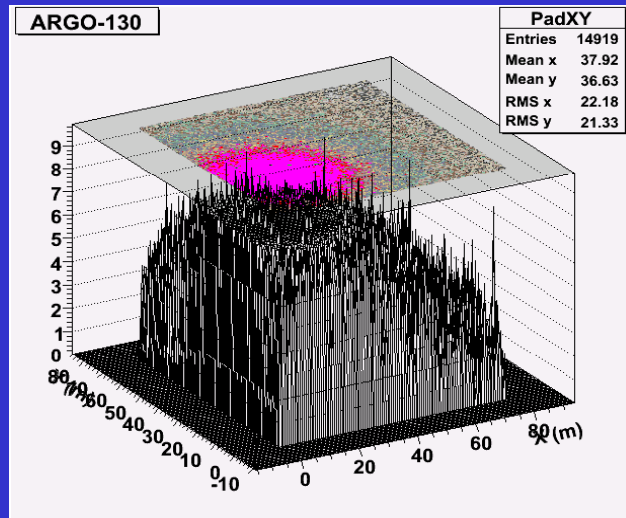
Look for detectable differences among various hadint models and data

Look for correlations with Xmax

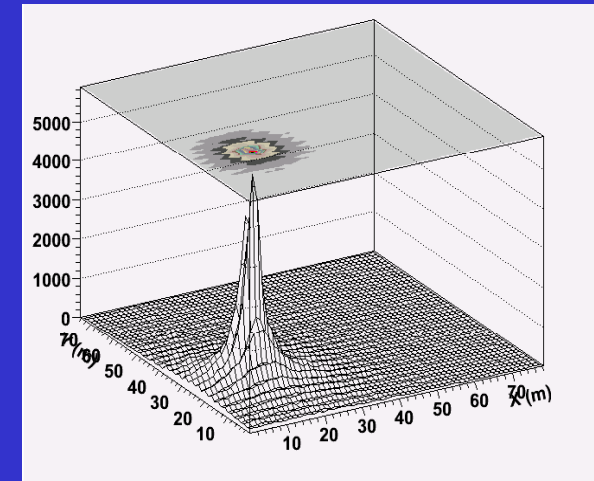


1 PeV simulated event

Digital
view

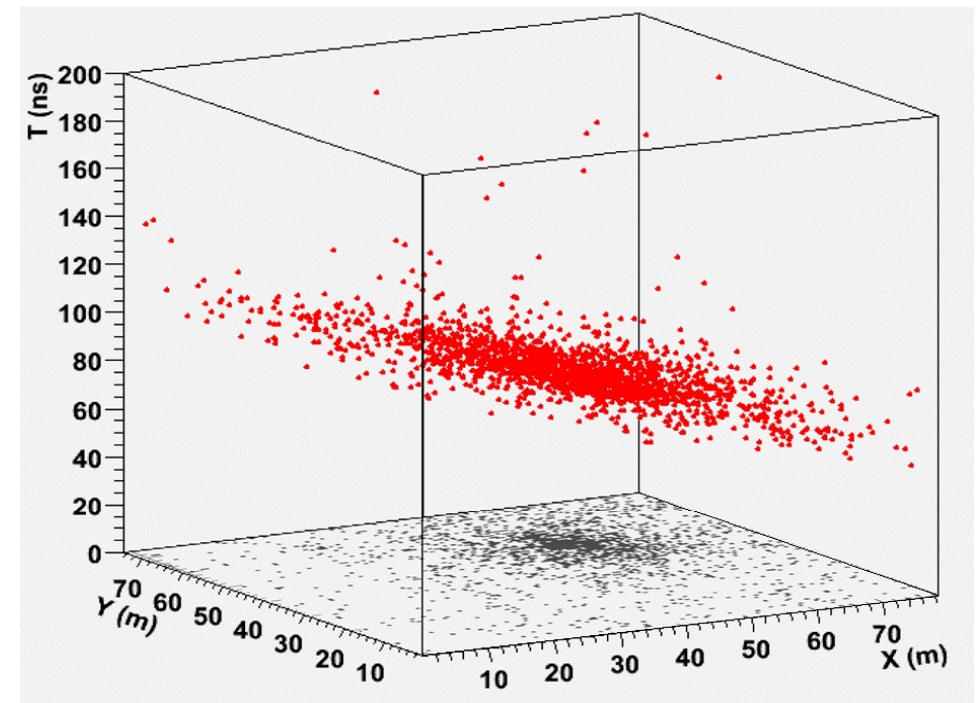
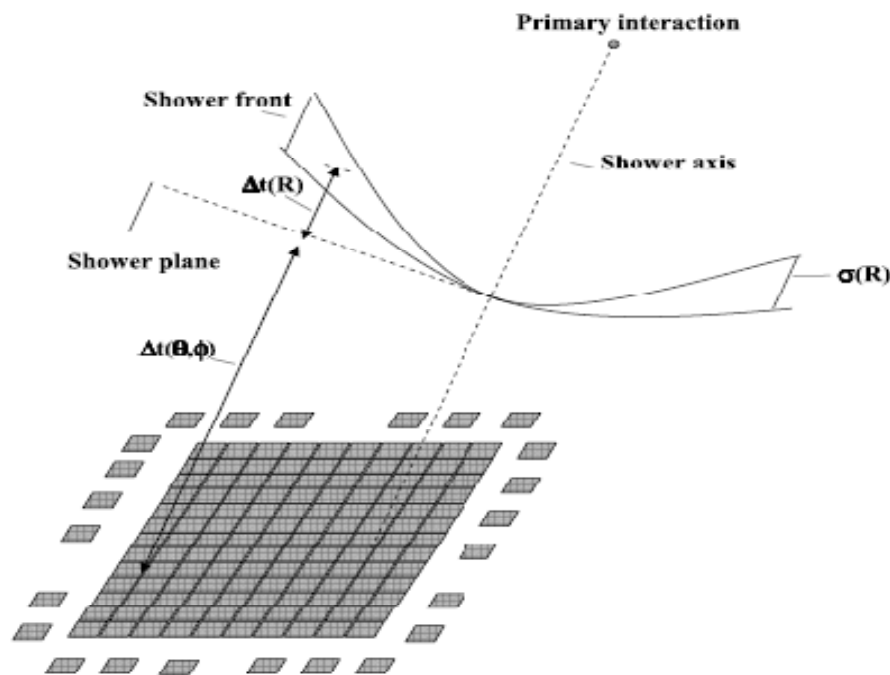


Analog
view



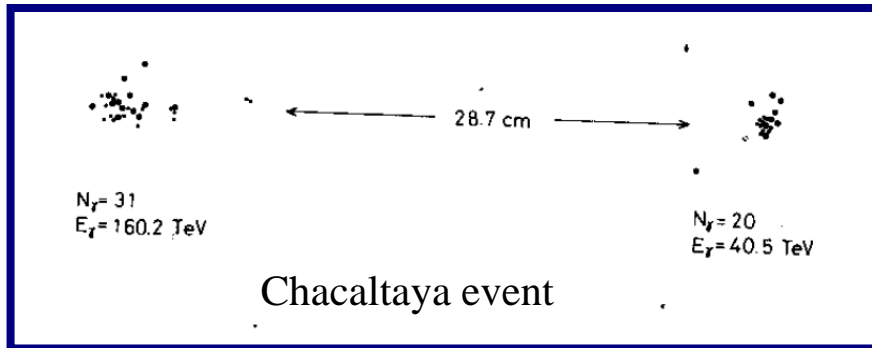
Shower front time structure

New observables are being studied, mainly **shape and width**, and their correlation with the longitudinal shower development

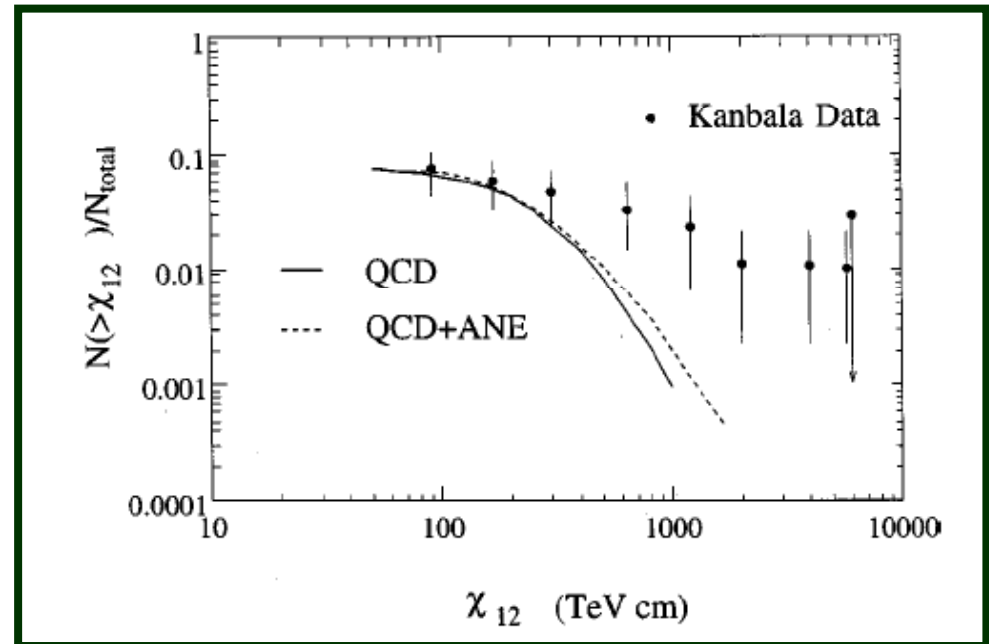


Multicore events

- They are correlated to large p_T jets
- Multicore γ –hadron family events in mountain emulsion experiments
- Events with $\chi_{12} = \sqrt{E_1 E_2} r_{12} \geq 1000 \text{TeVcm}$ still not explained by our present knowledge



Pamir Coll., Mt. Fuji Coll. and Chacaltaya Coll., Nucl. Phys. B191(1981)1-25



Z. Cao et al., Phys. Rev. D, v56 1997, 7361-7375

Exotic multicore events

PHYSICAL REVIEW D

VOLUME 52, NUMBER 5

1 SEPTEMBER 1995

Alignment in γ -hadron families of cosmic rays

V.V. Kopenkin,¹ A.K. Managadze,¹ I.V. Rakobolskaya,^{1,2} and T.M. Roganova¹

¹*Institute of Nuclear Physics, Moscow State University, Moscow 119899, Russia*

²*Department of Physics, Stanford University, Stanford, California 94305*

(Received 8 August 1994)

The alignment of the main fluxes of energy in a target plane is found in families of cosmic ray particles detected in deep lead x-ray chambers. The fraction of events with alignment is unexpectedly large for families with high energy and a large number of hadrons. This can be considered as evidence for the existence of coplanar scattering of secondary particles in the interaction of particles with superhigh energy, $E_0 \gtrsim 10^{16}$ eV. Data analysis suggests that the production of most aligned groups occurs slightly above the chamber and is characterized by a coplanar scattering and quasi-scaling spectrum of secondaries in the fragmentation region. The most elaborated hypothesis for the explanation of the alignment is related to the quark-gluon string rupture. However, the problem of the theoretical interpretation of our results still remains open.

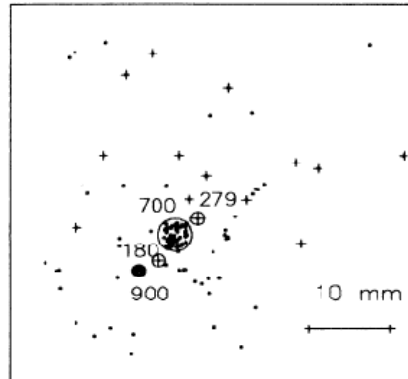


FIG. 2. An example of the target diagram with energy distinguished cores for the event with alignment (the family Pb-6). $\lambda_4=0.95$. Figures in the plot stand for energy in TeV (already multiplied by 3 for hadrons). EDC: \oplus is the halo of electromagnetic origin; \bullet is the hadronic halo; \otimes are the high energy hadrons; \bullet are the family γ quanta; + are the hadrons of the family.

A.DE Roeck et al., in arXiv:1002.3527

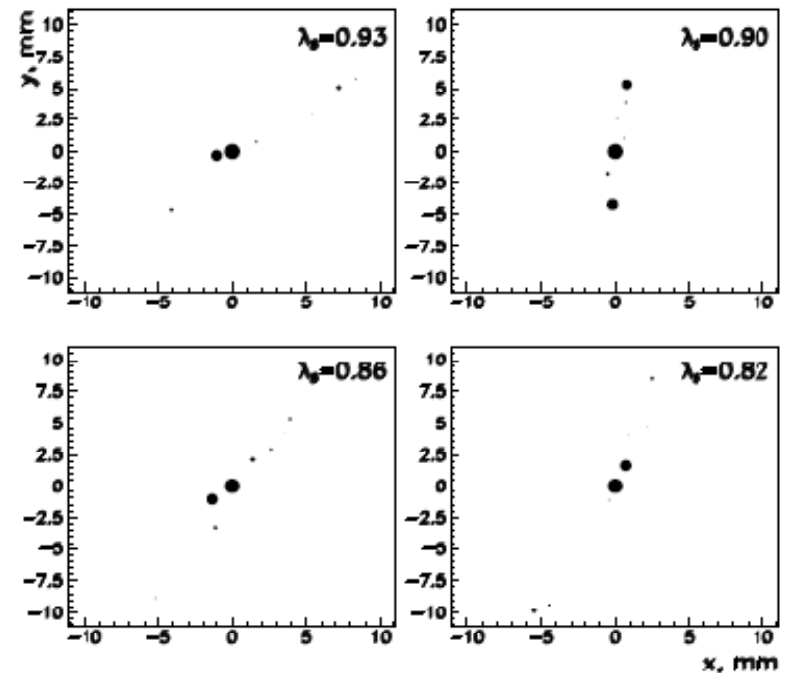


Figure 2: Samples of core distributions for PYTHIA simulated events with $E_{\Sigma}^{\text{thr}} = 10$ PeV and $\lambda_8 > 0.8$. The size of spots is proportional to their energy (except for the central spot which is not to scale).